Sulfate metabolites provide an intracellular pool for resveratrol generation and induce autophagy with senescence

Ketan R. Patel, Catherine Andreadi, Robert G. Britton, Emma Horner-Glister, Ankur Karmokar, Stewart Sale, Victoria A. Brown, Dean E. Brenner[1], Rajinder Singh, William P. Steward, Andreas J. Gescher and Karen Brown*

Department of Cancer Studies and Molecular Medicine, University of Leicester, Leicester, UK. [1]Departments of Internal Medicine and Pharmacology, University of Michigan Medical School and VA Medical Center, Ann Arbor, Michigan.

***To whom correspondence should be addressed:** Karen Brown, kb20@le.ac.uk.

One Sentence Summary: Biologically active concentrations of resveratrol can be generated intracellularly following uptake of the major human sulfate metabolites by selected cells; at doses considered safe in humans, resveratrol produced via this route may be of greater importance than unmetabolised resveratrol for eliciting beneficial effects.

Abstract:

The phytochemical resveratrol is thought to exert numerous health benefits. Its rapid phase II metabolism and resulting poor bioavailability may limit translation of these effects to humans. It is conceivable, but unproven, that metabolites contribute to activity *in vivo*, perhaps via hydrolysis of conjugates regenerating the parent. We present the first accurate quantitation of resveratrol sulfate and glucuronide conjugates in human plasma and tissue following repeated ingestion of resveratrol. Pharmacokinetic characterisation of a mixture of resveratrol-3- and 4′-*O*-sulfates in mice demonstrates that these metabolites are orally absorbed, but have low bioavailability at ~14 and 3%, respectively. Sulfate hydrolysis *in vivo*, liberates free resveratrol, which accounts for ~2% of the total resveratrol species present in plasma. Monosulfate metabolites were also converted to the parent in human colorectal cells. The extent of cellular uptake was dependent on specific membrane transporters and dictated anti-proliferative activity. Sulfate metabolites induced autophagy and senescence in cancer cells. These effects were abrogated by inclusion of a sulfatase inhibitor, which reduced intracellular resveratrol, suggesting the parent compound elicits this activity. These findings demonstrate that resveratrol sulfates may contribute to efficacy *in vivo*, by delivering resveratrol to target tissues in a stable conjugated form enabling gradual regeneration of the parent within selected cells. At doses considered safe in humans resveratrol generated via this route may be of greater importance than unmetabolised resveratrol.

Introduction

The phytochemical resveratrol (*trans*-3,5,4′-trihydroxystilbene) has been purported to have numerous health benefits. Preclinical evidence in model systems suggests resveratrol has cancer chemopreventive properties (*1*) and can impact upon cardiovascular (*2*) and neurodegenerative diseases (*3*), promote longevity of lower organisms (*4*), and delay or attenuate many age related changes and early mortality due to obesity in mice (*5*), (*6*). A wealth of mechanistic data supports the role of resveratrol in the management of these conditions by virtue of its anti-oxidant, anti-inflammatory, anti-tumorigenic and calorie restriction mimetic properties (*7*). However, a perceived major limitation in translating these observations to efficacy in humans is the fact that resveratrol is poorly bioavailable, due to rapid and extensive phase II metabolism, and toxicity concerns prohibit simply increasing the dose to overcome this issue (*8*). This is exemplified by our previous pharmacokinetic study in healthy volunteers, which revealed the prominent plasma and urinary species to be resveratrol-3-*O*-sulfate, resveratrol-3-*O*-glucuronide and resveratrol-4′-*O*-glucuronide, after a single dose of resveratrol (0.5-5.0 g) (*9*). The estimated total exposure to these metabolites, as indicated by the AUC_{inf}, was between 5-23-fold greater than the parent compound (*9*). Repeated ingestion of resveratrol at doses exceeding 1.0 g per day is associated with the occurrence of gastrointestinal side effects, which although mild, would certainly prohibit the long-term use of such doses in high-risk or healthy populations (*10*), (*11*). Consumption of 1.0 g resveratrol affords maximal plasma concentrations of ~0.6 μM in humans (*10*), but the majority of reported *in vitro* studies, particularly those relating to cancer, necessitate concentrations above this for detectable activity. This raises the question of whether sufficient levels of resveratrol can be safely attained in humans or whether resveratrol metabolites might contribute to the beneficial effects associated with resveratrol and negate this concern. It has long been speculated that resveratrol conjugates may themselves elicit biological changes, or may undergo hydrolysis *in vivo* to regenerate the parent compound (*12*); importantly, the ability of resveratrol metabolites to provide a reservoir of resveratrol has not yet been directly proven.

To date, no *in vivo* experiments and only a limited number of *in vitro* studies have attempted to address the potential effects of resveratrol metabolites. Conjugated derivatives of dietary polyphenols often have reduced

anti-proliferative activity compared to the parent compound, and this seems to be the case for resveratrol (*13*), (*14*). However, individual monosulfate metabolites have been found to possess comparable or greater potency than resveratrol against specific molecular targets, namely cyclooxygenase (COX), quinone reductase 1 (NQO1) and NFκβ, as well as a similar ability to scavenge free radicals (*15*), (*16*).

In this study we present the first accurate quantitation of conjugates in human plasma and colorectal tissue following repeated ingestion of resveratrol, which defines the concentration range suitable for preclinical investigations. After administration to mice, resveratrol-3- and 4′-*O*-sulfates were absorbed and hydrolysed, liberating free resveratrol in plasma and tissues. Intracellular conversion of monosulfate metabolites to the parent was directly confirmed in a panel of human colorectal cell lines, in which the extent of uptake dictated the degree of anti-proliferative activity and was dependent on the presence of specific membrane transporters. Pharmacologically achievable concentrations of sulfate metabolites were able to induce autophagy and senescence in cancer cells, which has broad implications for the management of a variety of chronic and age-related diseases. However, co-incubation with a sulfatase inhibitor abrogated the expression of autophagic and senescence markers, mirroring the reduction in intracellular resveratrol, which suggests the parent compound elicits this activity. These findings demonstrate that resveratrol sulfates may contribute appreciably to any efficacy observed *in vivo*, by providing a means of delivering resveratrol to target tissues in a more stable conjugated form, enabling gradual regeneration of the active parent within selected cells.

Results

Concentrations of resveratrol conjugates greatly exceed previous estimations

Acquisition of detailed human pharmacokinetic information is essential for the rational development of all pharmaceuticals and dietary agents, and may be especially valuable for resveratrol, with its numerous potential indications and wide ranging molecular targets. Optimal concentrations of the active species required for efficacy may vary considerably, depending on the disease being treated or intending to be prevented. Therefore, it is important that all resveratrol-derived species with biological activity are identified and accurate measurement of their plasma/tissue levels is obtained.

Due to the lack of available authentic standards, previous published investigations, including our own clinical pharmacokinetic studies, have been restricted to reporting estimated concentrations of the major resveratrol conjugates generated *in vivo* (*17*), (*10*). Such approximations are based on the use of a resveratrol standard curve, which is dependent on the extraction and spectroscopic characteristics of resveratrol itself. We have now synthesized sufficient quantities of resveratrol sulfate and glucuronide standards to enable reanalysis of a representative set of plasma and colorectal samples from our recent clinical trials involving repeated administration of resveratrol capsules to volunteers (*10*) and cancer patients (*17*), using our validated HPLC-UV assay (Figure 1). Standard curves used for the analysis were reproducible, with R^2 values ≥ 0.99 indicating linearity over the concentration range measured. The limit of quantitation was 10, 12 and 8 ng/ml for resveratrol-4'-*O*-glucuronide, resveratrol-4'-*O*-sulfate and resveratrol-3-*O*-sulfate, respectively.

Accurate determination using metabolite standard curves revealed the average maximum plasma concentrations (C_{max}) for the monoglucuronides, 4'-*O*-sulfate and 3-*O*-sulfates were actually ~2.6, 3.8 and 2.9-fold higher, respectively, than previously described (Figure 1C and Table S1A). This means that repeated oral dosing with 1 g daily can yield plasma concentrations of the major 3-*O*-sulfate in the region of ~22 μM (range 8-32 μM), whilst the monoglucuronides typically reach ~7-8 μM (range 2-18 μM) (Table S1B). Reanalysis of colorectal concentrations also indicated significant previous underestimation, although not as pronounced as plasma

(Table S2); true levels were 1.7-fold higher, with 3-*O*-sulfate concentrations in tissue originating from the right and left side of the colon averaging ~54 and 1 nmol/g respectively (overall range 0-638 nmol/g), following ingestion of 1 g resveratrol for 8 days prior to surgical resection. This discrepancy between matrices suggests that metabolites are extracted with an efficiency closer to that of resveratrol when isolated from tissues compared to plasma. Selected samples were also subject to LC-MS/MS analysis, which not only confirmed metabolite identity for the major products but revealed the presence of metabolites not formerly detected in human plasma or tissues, namely resveratrol trisulfate, a disulfate glucuronide plus dihydroresveratrol monosulfate and glucuronide (Figure 1B). Although observed by LC-MS/MS, the reduced metabolite dihydroresveratrol, was not detected by HPLC-UV, due to the limit of detection being ~1000 ng/mL, making the method at least 200-fold less sensitive for this particular derivative, and presumably its conjugates, than for resveratrol (*18*).

Resveratrol monosulfates regenerate resveratrol in mice

The synthetic scheme adopted for the production of resveratrol monosulfates afforded a 3:2 mixture of 3-*O*- and -4′-*O*-sulfates in good yield (99.49% purity, Figure S1). Since these are both clinically relevant the mixture was used for the pharmacokinetic studies and initial biological evaluation described in the present study. It was anticipated that any evidence of activity would provide justification to undertake the time consuming separation procedures required to isolate the individual isomers in sufficient quantities for future investigations (19). Pharmacokinetic profiling of resveratrol monosulfates when administered as the mixture to mice by gavage and intravenous injection revealed they are systemically absorbed by the oral route, but exhibit poor bioavailability, at ~14% for the 3-*O*-sulfate and 3% for resveratrol 4′-*O*-sulfate. This can be attributed, at least in part, to rapid metabolism; regardless of the route of administration the monosulfates were subject to secondary transformation, generating glucuronides plus a disulfate and most importantly, the parent resveratrol in plasma, intestinal mucosa, liver, lung and pancreas (Figures 2 and S2). Detection of abundant resveratrol-3-*O*-glucuronide in plasma and tissues is also consistent with de-conjugation of the sulfate isomers *in vivo*. After oral administration of the resveratrol sulfate mixture the peak plasma levels of resveratrol attained were

approximately 20% of the combined monosulfate C_{max} value. Although the fold difference was greater for the various organs examined, in which the highest resveratrol concentrations ranged from 13-110 times lower than the sulfates, this still represents a considerable degree of conversion (Table S3 and Figure S3). Furthermore, resveratrol was present in plasma and liver 6 h after dosing and persisted for as long as 24 h within intestinal mucosa, suggesting the potential for prolonged exposure when formed via this route. Although the average concentration of resveratrol in mouse mucosa increased at 6 h relative to the level at 2 h, it was not significantly higher; therefore, it is not possible to conclude whether this actually corresponds to a second peak of resveratrol generated within intestinal tissue, which may have been indicative of increased sulfatase activity.

In order to quantify the potential contribution of resveratrol regeneration via monosulfate intermediates to the measured plasma levels, an identical pharmacokinetic study was conducted in mice administered resveratrol itself (120 mg/kg). Following gavage dosing, resveratrol monosulfates accounted for 10.5% of the total resveratrol species present in plasma, based on AUC values (Table S4A). According to the previous sulfate pharmacokinetic study, parent resveratrol equates to 1.9% of the total plasma AUC_{all} in mice (Table S4A). Therefore, when resveratrol is taken orally it can be estimated that 10.5% will be converted to monosulfates, and 1.9% of this conjugated form will be hydrolysed back to resveratrol in the plasma. Overall, this represents ~0.2% of the initial resveratrol dose. Comparison of the plasma half-life of resveratrol when administered as the parent compound (11.0 h) or in sulfate form (2.1 h) suggests that conversion to sulfate conjugates, rather than elimination of resveratrol may be the rate limiting step (Table S4B).

Sulfate metabolites provide an intracellular reservoir of resveratrol

The propensity for human cells to liberate resveratrol from the sulfate conjugates was then assessed in a panel of colorectal cell lines. Monitoring of the monosulfate concentrations in culture medium (37°C, 5% CO_2) over the course of seven days by HPLC-UV analysis offered no evidence of hydrolysis to the parent resveratrol in the absence of cells. Moreover, both sulfates were stable under these conditions, with no significant change in resveratrol-3-*O*-sulfate and just a small reduction in resveratrol-4′-*O*-sulfate concentrations (from 20.4 ± 1.1 to

16.4 ± 1.1 μM). The malignant cell lines HCA-7 and HT-29 together with HCEC cells, which are derived from normal colonic epithelia, were then incubated with clinically achievable concentrations of the monosulfate mixture (75 μM) or resveratrol (10 μM) and the uptake kinetics and metabolite profile determined by analysis of the medium and intracellular contents. These concentrations were chosen to mimic the differential between plasma levels of resveratrol and total monosulfates, but were also governed by practical considerations and the balance between using a high enough concentration to maximise the chances of detecting intracellular resveratrol species, whilst avoiding significant toxicity, which would reduce the number of intact cells available for analysis. HT-29 cells appeared the most metabolically active, generating a sulfate glucuronide as the prominent metabolite, and smaller amounts of resveratrol-4′-*O*-glucuronide in medium after 24 h incubation with the monosulfates (Figure 3). The concentration of these metabolites, together with the disulfate and resveratrol-3-*O*-glucuronide which appeared subsequently, increased over seven days to the extent that the 3-*O*-sulfate accounted for only 3% of the total resveratrol species (Figure S4). However, resveratrol itself was not detected in the medium at any time point. HCA-7 cells produced a qualitatively similar pattern of metabolites in the media but the extent of conversion was less. In contrast, HCEC cells displayed minimal metabolic capacity, generating only trace amounts of extracellular resveratrol-3-*O* and -4′-*O*-glucuronide. This differential activity was also reflected in incubations containing resveratrol; in HT-29 and HCA-7 cells resveratrol was completely converted (<0.2% remaining) to monoglucuronides and the 3-*O*-sulfate within 24 h, whereas resveratrol remained the predominant species in medium from the normal epithelial cells, with the 4′-*O*-sulfate the only metabolite detectable (Figures 3 and S4).

Formation of metabolites implies resveratrol sulfates can cross cellular membranes, and this was confirmed by their presence within HT-29 and HCA-7 cells throughout the entire 7 days incubation with the sulfate mixture (Figure 4). More interestingly, despite its absence from medium, free resveratrol was also apparent at every time point in the cancer cells, albeit at relatively low levels, but was never reliably detected in extracts from HCECs. Maximal intracellular resveratrol concentrations were attained at 24 h and were approximately 3-fold higher in the HT-29 (0.16 ± 0.05 ng/mg) compared to the HCA-7 cells (0.05 ± 0.02 ng/mg), consistent with the

greater absorption of sulfates by the former. Sulfate entry into HCA-7 cells was rapid, reaching peak concentrations of 3.2 ng/mg (~10 μM) by 15 mins (for the 3-*O*-sulfate), but considerably higher levels were achieved in the HT-29 cells (14.6 ng/mg, or ~45 μM at 24 h). It seems that the lack of metabolites detected in HCEC media may be attributed to particularly poor uptake of the sulfates by these cells, as intracellular concentrations were consistently below the limit of quantitation (0.001 ng/mg).

Following exposure to resveratrol, maximal concentrations of the parent achieved were broadly similar in all three cell lines (0.01-0.02 ng/mg) but were vastly superseded in HT-29 and HCA-7 cells by the amount of 3-*O*-sulfate produced, with maximum levels reaching ~0.33 and 0.36 ng/mg, respectively (Figure 4). In contrast, peak 3-*O*-sulfate levels were only 4-fold higher than resveratrol concentrations in the normal HCEC cells, and beyond ~30 min resveratrol itself was the major species observed. It therefore appears that absorption of free resveratrol, as well as the sulfate conjugates, is restricted in HCEC cells compared to the malignant cells, although another contributing factor influencing the profile could be low expression of the sulfotransferases responsible for resveratrol conjugation and/or high expression of sulfatases. Whether this lack of resveratrol uptake and metabolism is representative of all non-cancer colon cells requires further investigation.

Sulfate uptake correlates with expression of specific membrane transporters

Whilst the passage of resveratrol across cell membranes can be achieved through both passive diffusion and active processes (20), sulfate conjugates are likely to necessitate a transport mechanism. Comparison of the basal gene expression profiles of candidate transporters in the three cell lines using an array format revealed significant variations that may explain the differences in sulfate uptake (Figures 5A and S5). Of the 84 genes analysed, eleven followed a pattern consistent with the sulfate kinetic data, with expression numerically decreasing in the rank order HT-29 > HCA-7 > HCEC, and the ΔCt value for at least one of the possible pairings being significantly different (Figure 5A). To date, four of these genes have been ascribed a role in small molecule drug transport and may conceivably influence uptake, whilst the remaining encode proteins required for the passage of other substrates such as glucose or nucleosides. Likely contenders based on known

cargo specificity are the organic anion transporter SLC22A9 and the organic anion transporting polypeptides (OATPs) SLCO1B1 and SLCO1B3. Analysis of OATP protein levels revealed that OATP1B3 mirrored the gene expression data, with higher levels in both cancer cell lines compared to HCEC cells (Figure 5B). In contrast, OATP1B1 protein was undetectable in all cell lines. When co-incubated with ursolic acid, a compound that inhibits both OATP1B1 and 1B3 but has greater selectivity for the latter (21), intracellular concentrations of resveratrol-3-*O*-sulfate were significantly reduced in HT-29 cells by 28 and 14% at 15 and 60 minutes, respectively. Whilst uptake of the 4′-*O*-sulfate was also impaired, the effect failed to reach significance. Overall, these results indicate that OATP1B3-mediated transport influences intracellular concentrations of resveratrol sulfates, although further experimental confirmation is needed.

Vesicular transport experiments have previously shown that resveratrol sulfates are a substrate for breast cancer resistance protein (BCRP, ABCG2), a member of the ATP binding cassette (ABC) superfamily of membrane transporters (22). ABCG2 was highly expressed in HT-29 cells, with mRNA levels over 350-fold greater than in HCA-7 cells, however, it was also present in the normal colon cell line at levels ~18 times higher than HCA-7 cells (Figure S5). The presence of ABCG2 would be expected to have a negative impact on intracellular concentrations given that ABC transporters are principally efflux proteins. However, expression of ABCG2 in HCEC cells may not actually contribute to the balance of influx/efflux as the kinetic studies (Figure 4) suggest that resveratrol sulfates fail to enter these cells to any measurable extent. The relatively higher expression of ABCG2 in HT-29 cells compared to HCA-7 directly contrasts with what might be predicted from the intracellular levels; this may indicate differences in uptake and/or the contribution of other efflux proteins overrides the effect of ABCG2.

Clinically relevant concentrations of resveratrol monosulfates attenuate cell growth through the induction of autophagy and senescence

The ability of clinically relevant levels of resveratrol monosulfates and glucuronide conjugates to inhibit the growth of colorectal cancer and normal epithelial cells was assessed over seven days and compared to the activity of resveratrol, at a concentration achievable in human colon (10 μM). Whilst both glucuronide conjugates had little effect on cell numbers, even at 250 μM, the mixture of monosulfates produced significant dose-dependent reduction at concentrations equal to or exceeding 25 μM for HCA-7 and 50 μM for HT-29 cancer cells (Figure 5D). Consistent with the relative intracellular concentrations, the most pronounced inhibition was evident in the HT-29 cells. Furthermore, the normal epithelial cell line HCEC, was completely unaffected by the presence of resveratrol sulfates over the dose range investigated, although resveratrol retained a degree of activity similar to that measured in HT-29 cells, causing a ~32% reduction.

The decreased cell numbers cannot entirely be explained by simple growth arrest or apoptosis, since a concentration approximating the IC_{50} in HT-29 cells (75 μM) failed to alter the distribution within each phase of the cell cycle over the course of 72 h, nor to significantly increase the extent of apoptosis or necrosis (Figure S6). Similarly, resveratrol at clinically attainable tissue concentrations (10 μM) was unable to induce significant death or arrest of HT-29 cells, as measured by propidium iodide staining, which does not distinguish between G_0 and G_1 phases of the cell cycle. As expected, considering the lack of effect on HCEC growth, there was no indication of sulfate-stimulated apoptosis, necrosis or arrest in these cells, even at a concentration of 250 μM.

Alternative processes that may contribute to the growth inhibition observed are autophagy, which is a lysosomal-dependent cellular catabolic pathway required for the quality control of proteins/organelles and maintenance of energy homeostasis, and senescence, a stable form of cell cycle arrest. Both programmes can be triggered by cellular stresses and serve as tumor suppressor mechanisms. Moreover, it has recently become apparent they are functionally intertwined (*23*), (*24*). Treatment of HT-29 cells for 24 h with the sulfate metabolites, but not resveratrol, significantly enhanced the conversion of soluble microtubule-associated protein 1 light chain 3 (LC3-I) to lipid bound LC3-II, a constituent of autophagosomal membranes and marker of autophagy initiation (Figure 5E & G). This activity was confirmed by transmission electron microscopy, which

revealed characteristic hallmarks of autophagy, including the presence of numerous vesicles with distinct double membranes (Figure 5I & J; (*25*)). The link between an antiproliferative effect, or lack thereof, and autophagy was further reinforced by the discovery that resveratrol sulfates failed to stimulate LC3-II production in HCEC cells (Figure S7). In addition, sulfate concentrations of 75 and 250 μM caused a persistent and significant up-regulation of p21 protein expression and amplified senescence-associated β-galactosidase (SA-β-gal) staining at pH 6.0, two established markers of senescence, in HT-29 cells, but not in the normal cell line (Figure S7). Conversely there was no discernible increase in cancer cells incubated with resveratrol itself at concentrations of 5 and 10 μM (Figure 5F-H), which may be explained by the lower levels of intracellular resveratrol species achieved (Figure 4, Table S5).

Autophagy and senescence induction are mediated by intracellular resveratrol

To ascertain the direct contribution of resveratrol sulfates to the activity observed *in vitro*, HT-29 cells were co-incubated with the metabolites (75 μM) and a non-toxic concentration of estrone 3-*O*-sulfamate (EMATE, STX64) a potent active site-directed inhibitor of steroid sulfatase (*26*). As predicted, EMATE inhibited the intracellular hydrolysis of resveratrol sulfates, significantly reducing conversion to resveratrol by 42% over 24 h, whilst elevating sulfate concentrations by ~31% (Figure 6A). Higher concentrations of EMATE were not associated with greater inhibition, implying that resveratrol sulfates serve as substrates for other sulfatase enzymes. Importantly, this shift in metabolite pattern was accompanied by a ~71% reduction in LC3-II accumulation relative to cells treated with the sulfates alone, and a ~34% decrease in p21 expression, although this latter effect was not significant. These observations strongly suggest the parent compound, rather than the sulfate conjugates, is responsible for inducing autophagy and possibly senescence (Figure 6).

Discussion

In recent years resveratrol has received considerable scientific and public attention for its numerous potential health benefits, but doubts persist over whether the promising preclinical data can translate to humans because of its rapid metabolism and resulting poor bioavailability (8). Whether the major products of this transformation, sulfate and glucuronide conjugates, can contribute to activity *in vivo* has important implications for the future clinical development of resveratrol, particularly whether the development of alternative prodrugs or drug-delivery systems that resist metabolism is indicated.

The mouse pharmacokinetic study presented here provides the first direct demonstration that resveratrol can be generated from its sulfate conjugates, and that formation via this route results in sustained exposure to the parent compound. Therefore, the potential exists for prolonged intracellular regeneration of the parent within internal target tissues for as long as these conjugates persist, which is at least 24 h for the 3-*O*-sulfate in human plasma (10). Irrespective of the actual species responsible, it is extremely encouraging that pharmacologically achievable concentrations of resveratrol sulfates, as defined in our clinical trials, induce favourable biological effects, namely growth inhibition through a combination of autophagy and senescence. Plasma sulfate concentrations of 20-30 μM can be attained in humans with repeated ingestion of 1 g resveratrol daily, which probably equates to the upper dose limit for prevention purposes based on resveratrol tolerability and safety (11). Concentrations within this range (25 μM) inhibited the proliferation of HT-29 and HCA-7 cancer cells by ~20%, whilst sparing the normal epithelium-derived HCEC cells. Moreover, the levels reached in human colorectal tissue originating from the right side of the intestine averaged 50 μM, but could reach as high as ~640 μM, which surpasses the concentrations required for 95% inhibition of HT-29 cell growth (250 μM).

Nothing is known about the metabolite profile of resveratrol in human tissues other than the colon, and in the absence of data to the contrary, it seems reasonable to assume that the blood supply will dictate the pattern, with phase II conjugates dominating in tissues distant to the gastrointestinal tract. Although this has long been considered a major limitation of resveratrol, the demonstration that sulfate metabolites are taken up into human

cells and can provide a reservoir for regenerating the parent *in situ*, suggests they contribute appreciably to the activity of this compound. Furthermore, it is feasible that intracellular resveratrol arising through this route may actually play a greater role than the unchanged parent *in vivo*, since the maximum concentration produced by incubation with 75 µM resveratrol sulfates was over 10-fold higher than that detected in cells treated with 10 µM resveratrol, a concentration that exceeds, by a factor of sixteen, that attainable in human plasma from a 1.0 g daily dose (10). These observations may also help explain how resveratrol is able to exert efficacy in numerous *in vivo* mouse models, which rely on systemic delivery to the target organ, such as suppression of pancreatic and prostate cancer (27), (28) protection against diet-induced metabolic heart disease (29) and delaying age-related deterioration (30), as well as emerging evidence from clinical trials showing resveratrol confers metabolic benefits in humans (31).

Other investigators have concluded that resveratrol sulfates are unable to affect the viability of SK-N-AS and NGP neuroblastoma cells (13). This inactivity was attributed to lack of uptake, as detected by fluorescence multiphoton microscopy, which measures the intrinsic fluorescence of resveratrol species. In contrast, individual resveratrol sulfates have some, albeit poor, cytotoxicity in breast cancer cell lines but are considerably less potent than resveratrol (32). These accounts may be rationalised by our finding that uptake of resveratrol sulfates is cell specific and dependent on the expression of certain transporters. SLCO1B3 seems to contribute to this process, although other members of the solute carrier (SLC) families such as SLC22A9, may also play a role (33). In colon cells, anti-proliferative activity correlated with the amount of resveratrol generated, which was governed by the efficiency of uptake of resveratrol sulfates. Whilst this may be the initial determining factor, it is also recognised that variations in sulfatase activity will impact on cellular response (34). Although only basal levels were assessed in this study, exposure to resveratrol derivatives may modulate expression or activity of membrane transporters over time (35). Many cancer tissues and cell lines have altered expression of OATPs; SLCO1B3for example, is normally liver-exclusive but is expressed at the mRNA and/or protein level in a variety of cancers, including colorectal adenocarcinomas (36), (37). This higher expression may render cancer cells more susceptible to the anti-proliferative effects of resveratrol, via sulfate

intermediates. The precise relevance of the anion transporters highlighted here in mediating resveratrol efficacy and their potential contribution to inter-individual variability in clinical response warrants future investigation.

In contrast to resveratrol sulfates, the few published studies plus our current findings have consistently shown the glucuronide conjugates to be ineffective (13). This extends beyond the context of cancer as illustrated by the fact that resveratrol itself causes cytotoxicity and has synergistic antiviral activity against human immunodeficiency virus (HIV)-1 infection when used in combination with nucleoside analogues, but the glucuronides had no impact, even at concentrations of 300 μM (14). Resveratrol glucuronides have relatively high affinity for multidrug resistance protein 3 (MRP3, ABCC3), and are also substrates for ABCG2, albeit with much lower affinity (22). Although both are expressed at the mRNA level in all three cell lines employed in the current study, ABC transporters are generally considered to be responsible for drug efflux, therefore, it is unclear whether their presence might aid or hinder activity in this model system. The complete lack of anti-proliferative effect tends to suggest that if taken up into cells, resveratrol glucuronides are either extremely rapidly pumped out, or are themselves inactive and fail to generate resveratrol at sufficient concentrations for activity. Kinetic studies analogous to those performed for resveratrol sulfates would help ascertain whether glucuronides play any role in resveratrol efficacy *in vivo* or are purely a clearance route.

The key finding that clinically achievable concentrations of resveratrol sulfates can induce autophagy and potentially senescence could have tremendous implications, given the diverse array of pathologies that these processes can impact on. The ability of resveratrol to stimulate autophagy is well recognised in experimental systems. It is thought to contribute to neuroprotection in animal models of Alzheimer's disease and Parkinson's disease, as well as attenuating human prion protein-mediated neurotoxicity and being universally required for the lifespan-prolonging effects of both caloric restriction and resveratrol (38), (39), (40), (41). Resveratrol displays hormetic behaviour on cardiomyocyte physiology, upregulating autophagy at low concentrations, which is associated with preservation of cardiac function during aging, whilst inhibiting the process at higher exposures (42).

The role of autophagy in carcinogenesis is paradoxical; it can act as an oncogenic or tumor supressing mechanism (43), and recent evidence supports a protective function for resveratrol in both settings (44), (45). Nevertheless, it should be noted that the concentrations used in these published accounts were beyond what can safely be achieved in human plasma, and presumably internal tissues. Consistent with the present study, where resveratrol sulfate-induced autophagy correlated with reduced cell numbers, resveratrol itself triggers autophagic cell death in chronic myelogenous leukaemia cells (44). Conversely, resveratrol can also enhance the therapeutic effect of temozolomide, an alkylating agent, through inhibition of autophagy in malignant glioma cells, thereby promoting apoptosis (45).

Autophagy has recently been identified as a new effector mechanism of senescence, important for the rapid protein remodelling needed to make the efficient transition from a proliferative to a senescent state (23). Senescence, which can be triggered by redox stress, DNA damage or oncogene activation, independently serves as a protective mechanism against cancer, arresting the growth of cells at risk for tumorigenesis and causing immune mediated clearance (46), (47). Whilst chronic exposure to resveratrol has previously been shown to induce senescence-like growth arrest of cancer cells *in vitro*, nothing is known about the potential role of its major metabolites (48). In the current study using clinically relevant concentrations, convincing evidence of senescence was only apparent in resveratrol sulfate-treated cells, which also displayed signs of autophagy. The fact that resveratrol itself failed to cause a significant effect can be attributed to the higher intracellular concentration arising as a consequence of sulfate deconjugation, relative to that achieved by incubating with resveratrol directly. This observation further reiterates the suggestion that resveratrol generated *in situ* may be of greater importance than the unchanged parent for eliciting efficacy in humans. Further investigations on the inter-dependency of autophagy and senescence in mediating the effects of resveratrol are warranted.

Although sulfatase inhibition experiments described above indicate that resveratrol, rather than the sulfate metabolites caused autophagy and senescence, it remains feasible that the conjugates have some intrinsic

properties. In the most comprehensive mechanistic assessment of resveratrol metabolites to date, Hoshino *et al*. reported that at least one of the five possible sulfates investigated could inhibit TNF-α-induced NFκβ, decrease the production of nitric oxide by nitric oxide synthase, and induce NQO1 activity (15). However, all these assays were cell-based and in most cases activity was attenuated relative to resveratrol, therefore, in the absence of information on intracellular concentrations and metabolism, it is not possible to dismiss resveratrol as the sole active species. Less debatable is the inhibitory activity of resveratrol monosulfates against cyclooxygenase enzymes, and free radical scavenging propensity of resveratrol-3-*O*-sulfate, since these effects were observed in sub-cellular *in vitro* systems, where the chances of hydrolysis are considerably lower (15). Generation of models in which all sulfatase activity is knocked down, using shRNA/siRNA strategies for example, may help ascertain whether these direct effects translate to intact human cells. In addition, more detailed mechanistic investigations, particularly at earlier time points than those studied here, are required to elucidate the underlying molecular changes responsible for the autophagy and senescence caused by exposure to resveratrol sulfate.

Resveratrol is one of those naturally occurring substances which have received considerable attention because of its remarkable pharmacological properties in preclinical systems. The findings described here suggest a coherent, albeit complicated mechanistic scenario which explains how the major resveratrol metabolites in humans may contribute to activity; this is particularly important for justifying the use of resveratrol in the prevention or treatment of systemic diseases, or those where the target tissue is distant to the gastrointestinal tract. Crucially, doses within what is currently thought to be a safe range for humans generate concentrations that are sufficient for biological activity. The observation that resveratrol is produced from sulfate metabolites *in vivo* and then persists in plasma and tissues, may help justify a reduced dosing schedule in future clinical trials, which would minimize the potential for toxicity. Although there is considerable commercial interest in developing resveratrol pro-drugs and delivery systems aimed at resisting metabolism, the results of this study suggest such formulations may not be necessary to deliver efficacious concentrations to target tissues. Overall, these data strongly support the ongoing and future clinical evaluation of resveratrol and may assist investigators

in obtaining ethical/regulatory approval for such studies as well as providing fundamental insight to help optimize trial design.

Materials and Methods

Resveratrol metabolites were synthesised according to adaptations of published methods (19), (49). Details of the clinical trials involving healthy volunteers and patients have been described previously (10), (17). Human plasma and colorectal mucosa samples were extracted and analysed using our validated HPLC-UV assay (9), (10), (17) or LC-MS/MS (18). Mouse studies were approved by Leicester University Ethical Review Panel and licensed by the UK Home Office. Bioavailability in mice was calculated by comparing AUC values after IV and IG administration of resveratrol sulfates. Cell cycle and apoptosis analysis was performed by flow cytometry. LC3I/II and p21 expression were determined by Western blotting and analysis of senescence in cultured cells utilised a senescence β-gal staining kit (Cell Signalling). Gene expression was measured using the RT^2 Profiler PCR Array - Human Drug Transporters (Qiagen). More details are provided in Supplementary Materials and Methods.

Supplementary Materials

Materials and Methods

Fig. S1. ^{1}H-NMR spectrum of resveratrol sulfate.

Fig. S2. Metabolite profile in mouse tissues after oral resveratrol sulfate.

Fig. S3. Metabolite pharmacokinetics in mice.

Fig. S4. Kinetics of resveratrol/metabolite formation in cell media.

Fig. S5. Expression of transporter genes.

Fig. S6. Cell cycle and apoptosis analysis.

Fig. S7. Autophagy and senescence markers in HCEC cells

References:

1. J. M. Pezzuto, Resveratrol as an Inhibitor of Carcinogenesis. *Pharmaceutical Biology* **46**, 443-573 (2008).

2. J. A. Baur and D. A. Sinclair, Therapeutic potential of resveratrol: the *in vivo* evidence. *Nature reviews. Drug discovery* **5**, 493-506 (2006).

3. A. Y. Sun, Q. Wang, A. Simonyi and G. Y. Sun, Resveratrol as a therapeutic agent for neurodegenerative diseases. *Mol Neurobiol* **41**, 375-383 (2010).

4. K. T. Howitz, K. J. Bitterman, H. Y. Cohen, D. W. Lamming, S. Lavu, J. G. Wood, R. E. Zipkin, P. Chung, A. Kisielewski, L. L. Zhang, B. Scherer and D. A. Sinclair, Small molecule activators of sirtuins extend Saccharomyces cerevisiae lifespan. *Nature* **425**, 191-196 (2003).

5. J. A. Baur, K. J. Pearson, N. L. Price, H. A. Jamieson, C. Lerin, A. Kalra, V. V. Prabhu, J. S. Allard, G. Lopez-Lluch, K. Lewis, P. J. Pistell, S. Poosala, K. G. Becker, O. Boss, D. Gwinn, M. Wang, S. Ramaswamy, K. W. Fishbein, R. G. Spencer, E. G. Lakatta, D. Le Couteur, R. J. Shaw, P. Navas, P. Puigserver, D. K. Ingram, R. de Cabo and D. A. Sinclair, Resveratrol improves health and survival of mice on a high-calorie diet. *Nature* **444**, 337-342 (2006).

6. M. Lagouge, C. Argmann, Z. Gerhart-Hines, H. Meziane, C. Lerin, F. Daussin, N. Messadeq, J. Milne, P. Lambert, P. Elliott, B. Geny, M. Laakso, P. Puigserver and J. Auwerx, Resveratrol improves mitochondrial function and protects against metabolic disease by activating SIRT1 and PGC-1alpha. *Cell* **127**, 1109-1122 (2006).

7. O. Vang, N. Ahmad, C. A. Baile, J. A. Baur, K. Brown, A. Csiszar, D. K. Das, D. Delmas, C. Gottfried, H. Y. Lin, Q. Y. Ma, P. Mukhopadhyay, N. Nalini, J. M. Pezzuto, T. Richard, Y. Shukla, Y. J. Surh, T. Szekeres, T. Szkudelski, T. Walle and J. M. Wu, What is new for an old molecule? Systematic review and recommendations on the use of resveratrol. *PLoS One* **6**, e19881 (2011).

8. L. Subramanian, S. Youssef, S. Bhattacharya, J. Kenealey, A. S. Polans and P. R. van Ginkel, Resveratrol: challenges in translation to the clinic-a critical discussion. *Clin Cancer Res* **16**, 5942-5948 (2010).

9. D. J. Boocock, G. E. Faust, K. R. Patel, A. M. Schinas, V. A. Brown, M. P. Ducharme, T. D. Booth, J. A. Crowell, M. Perloff, A. J. Gescher, W. P. Steward and D. E. Brenner, Phase I dose escalation pharmacokinetic study in healthy volunteers of resveratrol, a potential cancer chemopreventive agent. *Cancer Epidemiol Biomarkers Prev* **16**, 1246-1252 (2007).

10. V. A. Brown, K. R. Patel, M. Viskaduraki, J. A. Crowell, M. Perloff, T. D. Booth, G. Vasilinin, A. Sen, A. M. Schinas, G. Piccirilli, K. Brown, W. P. Steward, A. J. Gescher and D. E. Brenner, Repeat dose study of the cancer chemopreventive agent resveratrol in healthy volunteers: safety, pharmacokinetics, and effect on the insulin-like growth factor axis. *Cancer Res* **70**, 9003-9011 (2010).

11. K. R. Patel, E. Scott, V. A. Brown, A. J. Gescher, W. P. Steward and K. Brown, Clinical trials of resveratrol. *Ann N Y Acad Sci* **1215**, 161-169 (2011).

12. A. J. Gescher and W. P. Steward, Relationship between mechanisms, bioavailibility, and preclinical chemopreventive efficacy of resveratrol: a conundrum. *Cancer Epidemiol Biomarkers Prev* **12**, 953-957 (2003).

13. J. D. Kenealey, L. Subramanian, P. van Ginkel, S. Darjatmoko, M. Lindstrom, V. Somoza, S. Ghosh, Z. Song, R. Hsung, G. S. Kwon, K. Eliceiri, D. Albert and A. Polans, Resveratrol Metabolites Do Not Elicit Early Pro-apoptotic Mechanisms in Neuroblastoma Cells. *J Agric Food Chem* **59**, 4979-86 (2011).

14. L. X. Wang, A. Heredia, H. Song, Z. Zhang, B. Yu, C. Davis and R. Redfield, Resveratrol glucuronides as the metabolites of resveratrol in humans: characterization, synthesis, and anti-HIV activity. *J Pharm Sci* **93**, 2448-2457 (2004).

15. J. Hoshino, E. J. Park, T. P. Kondratyuk, L. Marler, J. M. Pezzuto, R. B. van Breemen, S. Mo, Y. Li and M. Cushman, Selective synthesis and biological evaluation of sulfate-conjugated resveratrol metabolites. *J Med Chem* **53**, 5033-5043 (2010).

16. B. Calamini, K. Ratia, M. G. Malkowski, M. Cuendet, J. M. Pezzuto, B. D. Santarsiero and A. D. Mesecar, Pleiotropic mechanisms facilitated by resveratrol and its metabolites. *Biochem J* **429**, 273-282 (2010).

17. K. R. Patel, V. A. Brown, D. J. Jones, R. G. Britton, D. Hemingway, A. S. Miller, K. P. West, T. D. Booth, M. Perloff, J. A. Crowell, D. E. Brenner, W. P. Steward, A. J. Gescher and K. Brown, Clinical pharmacology of resveratrol and its metabolites in colorectal cancer patients. *Cancer Res* **70**, 7392-7399 (2010).

18. D. J. Boocock, K. R. Patel, G. E. Faust, D. P. Normolle, T. H. Marczylo, J. A. Crowell, D. E. Brenner, T. D. Booth, A. Gescher and W. P. Steward, Quantitation of trans-resveratrol and detection of its metabolites in human plasma and urine by high performance liquid chromatography. *J Chromatogr B Analyt Technol Biomed Life Sci* **848**, 182-187 (2007).

19. C. Yu, Y. G. Shin, J. W. Kosmeder, J. M. Pezzuto and R. B. van Breemen, Liquid chromatography/tandem mass spectrometric determination of inhibition of human cytochrome P450 isozymes by resveratrol and resveratrol-3-sulfate. *Rapid Commun Mass Spectrom* **17**, 307-313 (2003).

20. A. Lancon, D. Delmas, H. Osman, J. P. Thenot, B. Jannin and N. Latruffe, Human hepatic cell uptake of resveratrol: involvement of both passive diffusion and carrier-mediated process. *Biochem Biophys Res Commun* **316**, 1132-1137 (2004).

21. C. Gui, A. Obaidat, R. Chaguturu and B. Hagenbuch, Development of a cell-based high-throughput assay to screen for inhibitors of organic anion transporting polypeptides 1B1 and 1B3. *Curr Chemical Genomics* **4**, 1-8 (2010).

22. K. van de Wetering, A. Burkon, W. Feddema, A. Bot, H. de Jonge, V. Somoza and P. Borst, Intestinal breast cancer resistance protein (BCRP)/Bcrp1 and multidrug resistance protein 3 (MRP3)/Mrp3 are involved in the pharmacokinetics of resveratrol. *Mol Pharmacol* **75**, 876-885 (2009).

23. A. R. Young, M. Narita, M. Ferreira, K. Kirschner, M. Sadaie, J. F. Darot, S. Tavare, S. Arakawa, S. Shimizu, F. M. Watt and M. Narita, Autophagy mediates the mitotic senescence transition. *Genes & Development* **23**, 798-803 (2009).

24. A. R. Young and M. Narita, Connecting autophagy to senescence in pathophysiology. *Current Opinion in Cell Biology* **22**, 234-240 (2010).

25. E. L. Eskelinen, To be or not to be? Examples of incorrect identification of autophagic compartments in conventional transmission electron microscopy of mammalian cells. *Autophagy* **4**, 257-260 (2008).

26. L. W. L. Woo, C. Burbert, O.B. Sutcliffe, A. Smith, S. K. Chander, M. F. Mahon, A. Purohit, M. J. Reed and B. V. Potter, Dual aromatase-steroid sulfatase inhibitors. *J Med Chem* **50**, 3540-3560 (2007).

27. S. K. Roy, Q. Chen, J. Fu, S. Shankar and R. K. Srivastava, Resveratrol inhibits growth of orthotopic pancreatic tumors through activation of FOXO transcription factors. *PLoS One* **6**, e25166 (2011).

28. C. E. Harper, L. M. Cook, B. B. Patel, J. Wang, I. A. Eltoum, A. Arabshahi, T. Shirai and C. A. Lamartiniere, Genistein and resveratrol, alone and in combination, suppress prostate cancer in SV-40 tag rats. *The Prostate* **69**, 1668-1682 (2009).

29. F. Qin, D. A. Siwik, I. Luptak, X. Hou, L. Wang, A. Higuchi, R. M. Weisbrod, N. Ouchi, V. H. Tu, T. D. Calamaras, E. J. Miller, T. J. Verbeuren, K. Walsh, R. A. Cohen and W. S. Colucci, The polyphenols resveratrol and S17834 prevent the structural and functional sequelae of diet-induced metabolic heart disease in mice. *Circulation* **125**, 1757-1764, S1751-1756 (2012).

30. K. J. Pearson, J. A. Baur, K. N. Lewis, L. Peshkin, N. L. Price, N. Labinskyy, W. R. Swindell, D. Kamara, R. K. Minor, E. Perez, H. A. Jamieson, Y. Zhang, S. R. Dunn, K. Sharma, N. Pleshko, L. A. Woollett, A. Csiszar, Y. Ikeno, D. Le Couteur, P. J. Elliott, K. G. Becker, P. Navas, D. K. Ingram, N. S. Wolf, Z. Ungvari, D. A. Sinclair and R. de Cabo, Resveratrol delays age-related deterioration and mimics transcriptional aspects of dietary restriction without extending life span. *Cell Metabolism* **8**, 157-168 (2008).

31. S. Timmers, E. Konings, L. Bilet, R. H. Houtkooper, T. van de Weijer, G. H. Goossens, J. Hoeks, S. van der Krieken, D. Ryu, S. Kersten, E. Moonen-Kornips, M. K. Hesselink, I. Kunz, V. B. Schrauwen-Hinderling, E. E. Blaak, J. Auwerx and P. Schrauwen, Calorie restriction-like effects of 30 days of resveratrol supplementation on energy metabolism and metabolic profile in obese humans. *Cell Metabolism* **14**, 612-622 (2011).

32. M. Miksits, K. Wlcek, M. Svoboda, O. Kunert, E. Haslinger, T. Thalhammer, T. Szekeres and W. Jager, Antitumor activity of resveratrol and its sulfated metabolites against human breast cancer cells. *Planta Med* **75**, 1227-1230 (2009).

33. M. Roth, A. Obaidat and B. Hagenbuch, OATPs, OATs and OCTs: the organic anion and cation transporters of the SLCO and SLC22A gene superfamilies. *British Journal of Pharmacology* **165**, 1260-1287 (2012).

34. M. Miksits, K. Wlcek, M. Svoboda, T. Thalhammer, I. Ellinger, G. Stefanzl, C. N. Falany, T. Szekeres and W. Jaeger, Expression of sulfotransferases and sulfatases in human breast cancer: impact on resveratrol metabolism. *Cancer Lett* **289**, 237-245 (2010).

35. S. Shankar, D. Nall, S. N. Tang, D. Meeker, J. Passarini, J. Sharma and R. K. Srivastava, Resveratrol inhibits pancreatic cancer stem cell characteristics in human and KrasG12D transgenic mice by inhibiting pluripotency maintaining factors and epithelial-mesenchymal transition. *PLoS One* **6**, e16530 (2011).

36. W. Lee, A. Belkhiri, A. C. Lockhart, N. Merchant, H. Glaeser, E. I. Harris, M. K. Washington, E. M. Brunt, A. Zaika, R. B. Kim and W. El-Rifai, Overexpression of OATP1B3 confers apoptotic resistance in colon cancer. *Cancer Res* **68**, 10315-10323 (2008).

37. A. Obaidat, M. Roth and B. Hagenbuch, The expression and function of organic anion transporting polypeptides in normal tissues and in cancer. *Annual Review of Pharmacology and Toxicology* **52**, 135-151 (2012).

38. V. Vingtdeux, L. Giliberto, H. Zhao, P. Chandakkar, Q. Wu, J. E. Simon, E. M. Janle, J. Lobo, M. G. Ferruzzi, P. Davies and P. Marambaud, AMP-activated protein kinase signaling activation by resveratrol modulates amyloid-beta peptide metabolism. *J Biol Chem* **285**, 9100-9113 (2010).

39. Y. Wu, X. Li, J. X. Zhu, W. Xie, W. Le, Z. Fan, J. Jankovic and T. Pan, Resveratrol-activated AMPK/SIRT1/autophagy in cellular models of Parkinson's disease. *Neuro-Signals* **19**, 163-174 (2011).

40. J. K. Jeong, M. H. Moon, B. C. Bae, Y. J. Lee, J. W. Seol, H. S. Kang, J. S. Kim, S. J. Kang and S. Y. Park, Autophagy induced by resveratrol prevents human prion protein-mediated neurotoxicity. *Neuroscience Research* **73**, 99-105 (2012).

41. E. Morselli, M. C. Maiuri, M. Markaki, E. Megalou, A. Pasparaki, K. Palikaras, A. Criollo, L. Galluzzi, S. A. Malik, I. Vitale, M. Michaud, F. Madeo, N. Tavernarakis and G. Kroemer, Caloric restriction and resveratrol promote longevity through the Sirtuin-1-dependent induction of autophagy. *Cell Death & Disease* **1**, e10 (2010).

42. D. Dutta, R. Calvani, R. Bernabei, C. Leeuwenburgh and E. Marzetti, Contribution of impaired mitochondrial autophagy to cardiac aging: mechanisms and therapeutic opportunities. *Circulation Research* **110**, 1125-1138 (2012).

43. M. Hoare, A. R. Young and M. Narita, Autophagy in cancer: having your cake and eating it. *Seminars in Cancer Biology* **21**, 397-404 (2011).

44. A. Puissant, G. Robert, N. Fenouille, F. Luciano, J. P. Cassuto, S. Raynaud and P. Auberger, Resveratrol promotes autophagic cell death in chronic myelogenous leukemia cells via JNK-mediated p62/SQSTM1 expression and AMPK activation. *Cancer Res* **70**, 1042-1052 (2010).

45. C. J. Lin, C. C. Lee, Y. L. Shih, T. Y. Lin, S. H. Wang, Y. F. Lin and C. M. Shih, Resveratrol enhances the therapeutic effect of temozolomide against malignant glioma in vitro and in vivo by inhibiting autophagy. *Free Radic Biol Med* **52**, 377-391 (2012).

46. J. Campisi, Cellular senescence as a tumor-suppressor mechanism. *Trends in Cell Biology* **11**, S27-31 (2001).

47. T. W. Kang, T. Yevsa, N. Woller, L. Hoenicke, T. Wuestefeld, D. Dauch, A. Hohmeyer, M. Gereke, R. Rudalska, A. Potapova, M. Iken, M. Vucur, S. Weiss, M. Heikenwalder, S. Khan, J. Gil, D. Bruder, M. Manns, P. Schirmacher, F. Tacke, M. Ott, T. Luedde, T. Longerich, S. Kubicka and L. Zender, Senescence surveillance of pre-malignant hepatocytes limits liver cancer development. *Nature* **479**, 547-551 (2011).

48. E. H. Heiss, Y. D. Schilder and V. M. Dirsch, Chronic treatment with resveratrol induces redox stress-and ataxia telangiectasia-mutated (ATM)-dependent senescence in p53-positive cancer cells. *J Biol Chem* **282**, 26759-26766 (2007).

49. R. Lucas, D. Alcantara and J. C. Morales, A concise synthesis of glucuronide metabolites of urolithin-B, resveratrol, and hydroxytyrosol. *Carbohydrate Research* **344**, 1340-1346 (2009).

Acknowledgments: We thank Stefan Hyman and Natalie Allcock (University of Leicester) for electron microscopy assistance and Dr Atul Purohit (Imperial College London) for advice on the sulfatase inhibition experiments.

Funding: Supported by a Cancer Research UK programme (C325/A6691) with assistance from the Leicester Experimental Cancer Medicine Centre (C325/A15575, funded by Cancer Research UK/UK Department of Health) and US National Cancer Institute (NCI-N01-CN-25025).

Author contributions: K.R.P., C.A., R.G.B., E. H-G., R.S. and K.B. designed and/or performed all laboratory experiments; K.R.P., A.K. and S.S. performed *in vivo* studies; K.R.P, K.B., C.A., E. H-G., R.G.B., A.K. and A.G. analyzed the data; V.A.B., D.E.B, W.P.S. and A.G. designed and/or conducted clinical trials; K.B., A.G., W.P.S. and D.E.B. provided funding; K.B. and K.R.P. wrote the paper.

Fig. 1: **Resveratrol and its metabolites in human plasma and colorectal tissue.** (**A**) Representative HPLC-UV chromatograms of (**Ai**) plasma taken 1 h after the last dose from a healthy volunteer who received resveratrol (1.0 g) daily for 29 days, (**Aii**) colorectal cancer tissue from a patient that ingested 1.0 g resveratrol daily for eight days prior to surgery and (**Aiii**) authentic resveratrol and metabolite standards. Peaks were assigned by comparison of retention times with synthetic standards, where available, and the identity confirmed by LC-MS/MS in negative ionization mode. (**B**) Representative analysis of plasma extracts by LC-MS/MS with multiple reaction monitoring for the m/z transitions designated. Plasma was taken from a healthy volunteer 1.5 h post-dosing with 5 g of resveratrol on a day during the last week of a 29 day intervention. Where multiple peaks are present for a transition, asterisks indicate the peak of interest. Metabolites not previously identified in human plasma are in bold and underlined. (**C**) Concentration of resveratrol and its metabolites in human plasma estimated using resveratrol as standard (resveratrol equivalents, left) or accurately measured using synthetic metabolite standards (right). Healthy volunteers received resveratrol (0.5, 1.0, 2.5 or 5.0 g) daily for 29 days (*10*). Concentrations were determined by HPLC-UV analysis of plasma taken on a day during the last week of intervention. Values are the mean (+ SD) maximum plasma concentrations (C_{max}) for 3 randomly selected individuals per dose group.

Fig. 2: Resveratrol sulfates generate resveratrol *in vivo*. Representative HPLC-UV chromatograms of extracts of plasma (**B & C**) or mucosa (**D**) taken 1 h post-dosing from mice that received 120 mg/kg resveratrol (**B**) or resveratrol sulfates (3-*O*-sulfate and 4′-*O*-sulfate in a 3:2 ratio) (**C & D**) intragastrically. Chromatogram (**A**) shows the resveratrol sulfate mixture used for dosing. Metabolites were identified by comparison with synthetic standards, where available, and confirmed by LC-MS/MS. The internal standard (IS) is naringenin. Graphs (**a**) and (**b**) show 24 h kinetic profiles of resveratrol generated in plasma and mucosa respectively (mean + SD, 3 mice per time point) following administration of resveratrol sulfates.

Fig. 3: Resveratrol sulfates are deconjugated and glucuronidated in colorectal cells. Representative HPLC-UV chromatograms of extracts of cell medium from 24 h incubations with HCA-7 (**A, D**), HT-29 (**B, E**), or HCEC (**C, F**) cells containing either a 3:2 mixture of resveratrol-3-*O*- and -4′-*O*-sulfate (75 μM) (**A**-**C**) or resveratrol (10 μM) (**D**-**E**).

Fig. 4: Intracellular generation of resveratrol from resveratrol sulfates in human colorectal cells. Representative HPLC-UV chromatograms of extracts of HCA-7 (**A, D**), HT-29 (**B, E**), or HCEC (**C, F**) cells obtained from 24 h incubations containing either a 3:2 mixture of resveratrol-3-*O*- and -4′-*O*-sulfate (75 μM) or resveratrol (10 μM). Graphs (**1**) and (**2**) show the change in intracellular resveratrol-related species following incubation with the sulfate mixture over seven days. Intracellular concentrations in HCEC cells were below the limit of quantitation and are not shown. Graphs (**3**), (**4**) and (**5**) show the change in intracellular resveratrol-related species following incubation with 10 μM resveratrol. Comparison of intracellular resveratrol concentrations achieved in each of the three cell lines over time, following incubation with resveratrol sulfates or resveratrol (**G**). Error bars indicate SD, n=3 experiments.

Fig. 5: Resveratrol sulfates have selective antiproliferative activity, which correlates with membrane transporter expression. (**A**) Comparison of the basal expression of drug transporter genes in cells, determined using an RT^2 Profiler PCR array. Chart shows those genes for which the relative expression profile correlates with resveratrol sulfate uptake (i.e. HT-29 >HCA-7 >HCEC) and where significant differences ($p<0.01$, Two-Way ANOVA) were detected in ΔCt value between at least one of the possible pairings. Experiments were conducted in triplicate and data expressed relative to levels in HCA-7 cells (set as 1.0). *Indicates where expression in HCA-7 cells is significantly different from HT-29 or HCEC cells, # designates genes expressed at significantly higher levels in HT-29 compared to HCEC cells. (**B**) Basal protein expression of OATP1B1 and 1B3 in cell lines (100 μg protein loaded); positive control is HepG2 cell lysate (25 μg). (**C**) Effect of ursolic acid (+UA) co-incubation on resveratrol sulfate uptake in HT-29 cells (mean+SD, n=3, *significant decrease compared to control $p \leq 0.05$). (**D**) Proportion of cells remaining, relative to control, following incubation with

resveratrol sulfates (black) or resveratrol (green) for seven days (mean+SD of three experiments, performed in triplicate). *Indicates significant reduction compared to control ($p \leq 0.0005$, One-Way ANOVA). (**E-G**) Expression of LC3-I/II and p21 proteins in HT-29 cells incubated with resveratrol (green) or resveratrol sulfate mixture (black) for up to 72 h, measured by Western blotting. Signficant increases compared to control are indicated by $*p \leq 0.05$ and $**p = 0.01$ (Student's t-test). (**H**) Treatment with resveratrol sulfates (black) significantly increased SA-β-galactosidase activity in HT-29 cells measured at 72 h ($*p = 0.02$, $**p = 0.002$) but resveratrol (green) had no significant effect. Data in (**E**), (**F**) and (**H**) are the mean+SEM of three experiments. (**I-J**) Representative electron microscopy images of HT-29 cells incubated with 250 μM monosulfates (**I**) or vehicle (**J**) for 72 h. Arrows illustrate autophagosomes, late stage autophagic compartments and autolysosomes. Normal-looking nucleus (N) and mitochondria (M) are indicated. Magnifications for treated and control cells are 25,000x and 30,000x respectively.

Fig. 6: Autophagy is mediated by intracellular resveratrol. Effects of sulfatase inhibitor EMATE on intracellular generation of resveratrol (**A**) and LC3-I/II and p21 levels (**B-D**). HT-29 cells were incubated with EMATE (50 μM) for 1 h, after which resveratrol sulfates (75 μM of 3-*O*- and 4′-*O*-sulfate, 3:2 mixture) were added, and incubations terminated 24 h later. (**A**) Generation of resveratrol in cell pellets was determined by HPLC-UV analysis. Bars indicate mean±SD of four experiments, $*p < 0.0001$ (Student's T-test). (**B**) Representative Western blot of lysates from cells incubated with resveratrol sulfates in the presence/absence of EMATE. Densitometric quantitiation of LC3-II (**C**) and p21 (**D**) protein levels (mean+SEM, n=3 experiments). *Indicates significant difference between values obtained with/without EMATE (Student's T-test).

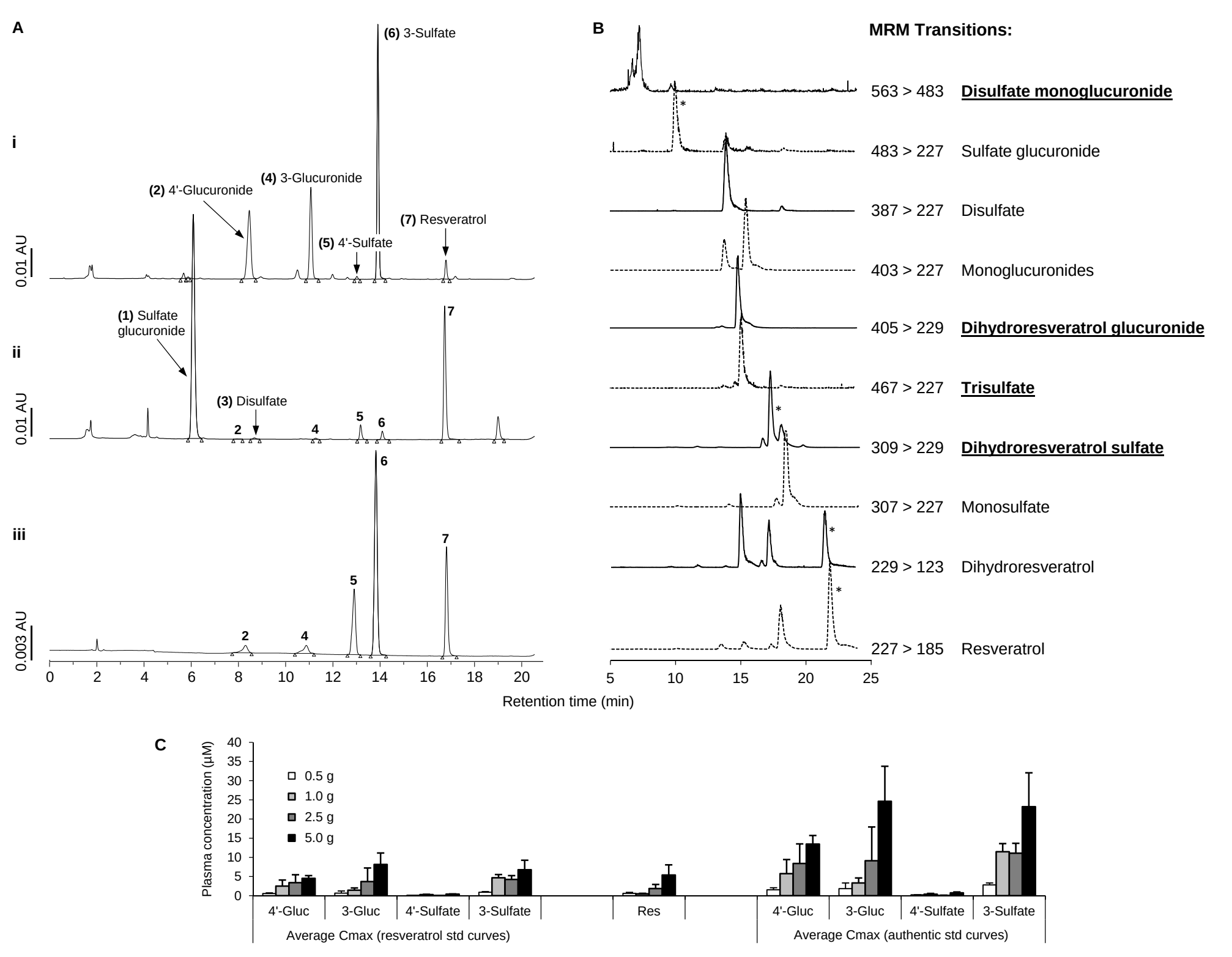
A
i
ii
iii
(6) 3-Sulfate
(2) 4'-Glucuronide
(4) 3-Glucuronide
(7) Resveratrol
(5) 4'-Sulfate
0.01 AU
(1) Sulfate glucuronide
(3) Disulfate
0.01 AU
0.003 AU
0 2 4 6 8 10 12 14 16 18 20
Retention time (min)
B
MRM Transitions:
563 > 483 Disulfate monoglucuronide
483 > 227 Sulfate glucuronide
387 > 227 Disulfate
403 > 227 Monoglucuronides
405 > 229 Dihydroresveratrol glucuronide
467 > 227 Trisulfate
309 > 229 Dihydroresveratrol sulfate
307 > 227 Monosulfate
229 > 123 Dihydroresveratrol
227 > 185 Resveratrol
5 10 15 20 25
C
Plasma concentration (μM)
0.5 g
1.0 g
2.5 g
5.0 g
4'-Gluc
3-Gluc
4'-Sulfate
3-Sulfate
Res
Average Cmax (resveratrol std curves)
Average Cmax (authentic std curves)

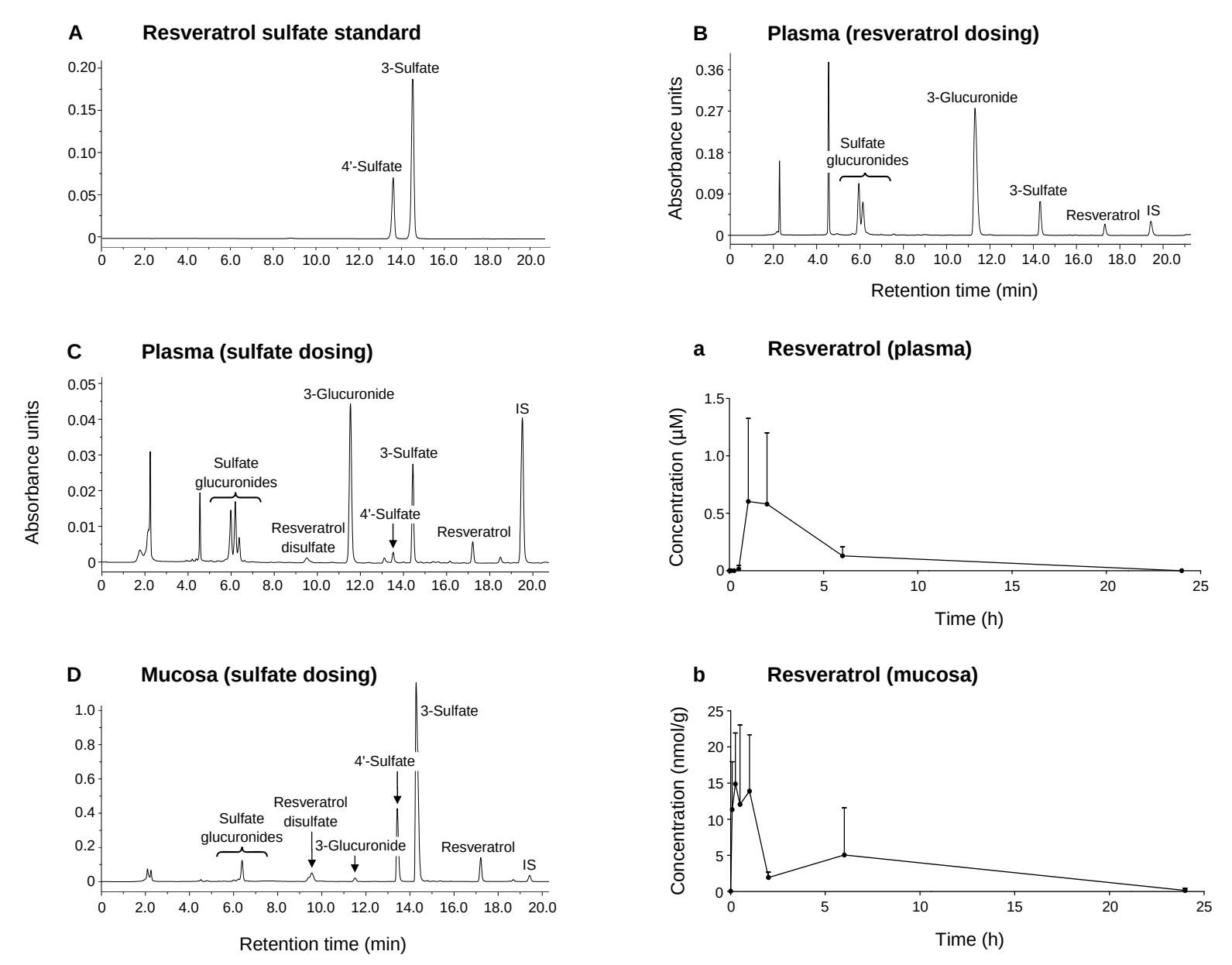
A
Resveratrol sulfate standard
3-Sulfate
4'-Sulfate
B
Plasma (resveratrol dosing)
Absorbance units
3-Glucuronide
Sulfate glucuronides
3-Sulfate
Resveratrol
IS
Retention time (min)
C
Plasma (sulfate dosing)
Absorbance units
3-Glucuronide
IS
Sulfate glucuronides
3-Sulfate
4'-Sulfate
Resveratrol disulfate
Resveratrol
a
Resveratrol (plasma)
Concentration (μM)
Time (h)
D
Mucosa (sulfate dosing)
3-Sulfate
4'-Sulfate
Resveratrol disulfate
Sulfate glucuronides
3-Glucuronide
Resveratrol
IS
Retention time (min)
b
Resveratrol (mucosa)
Concentration (nmol/g)
Time (h)

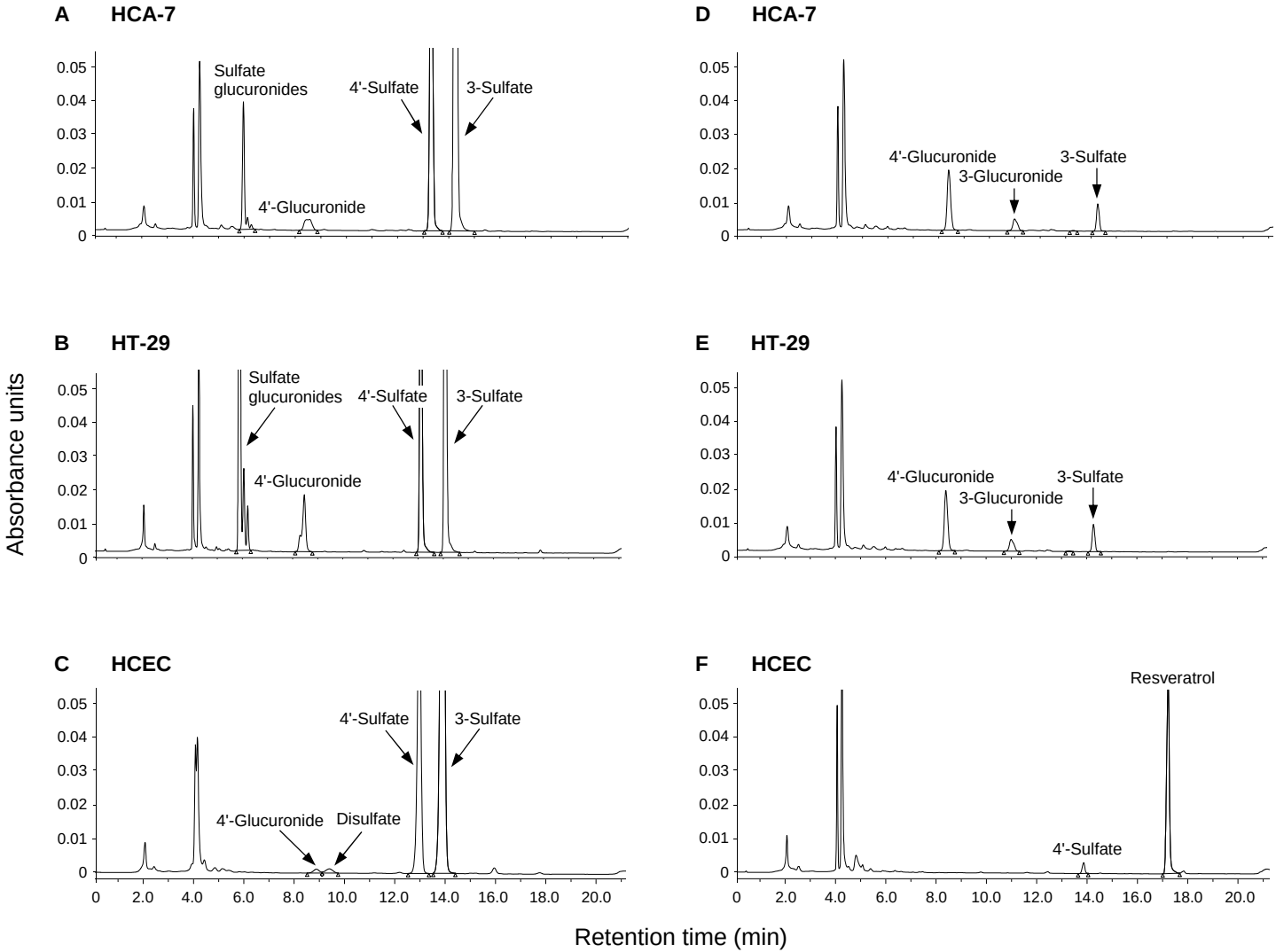
Resveratrol monosulfate incubations
Resveratrol incubations
A HCA-7
B HT-29
C HCEC
D HCA-7
E HT-29
F HCEC
Sulfate glucuronides
4'-Sulfate
3-Sulfate
4'-Glucuronide
Disulfate
4'-Glucuronide
3-Glucuronide
3-Sulfate
Resveratrol
Absorbance units
Retention time (min)

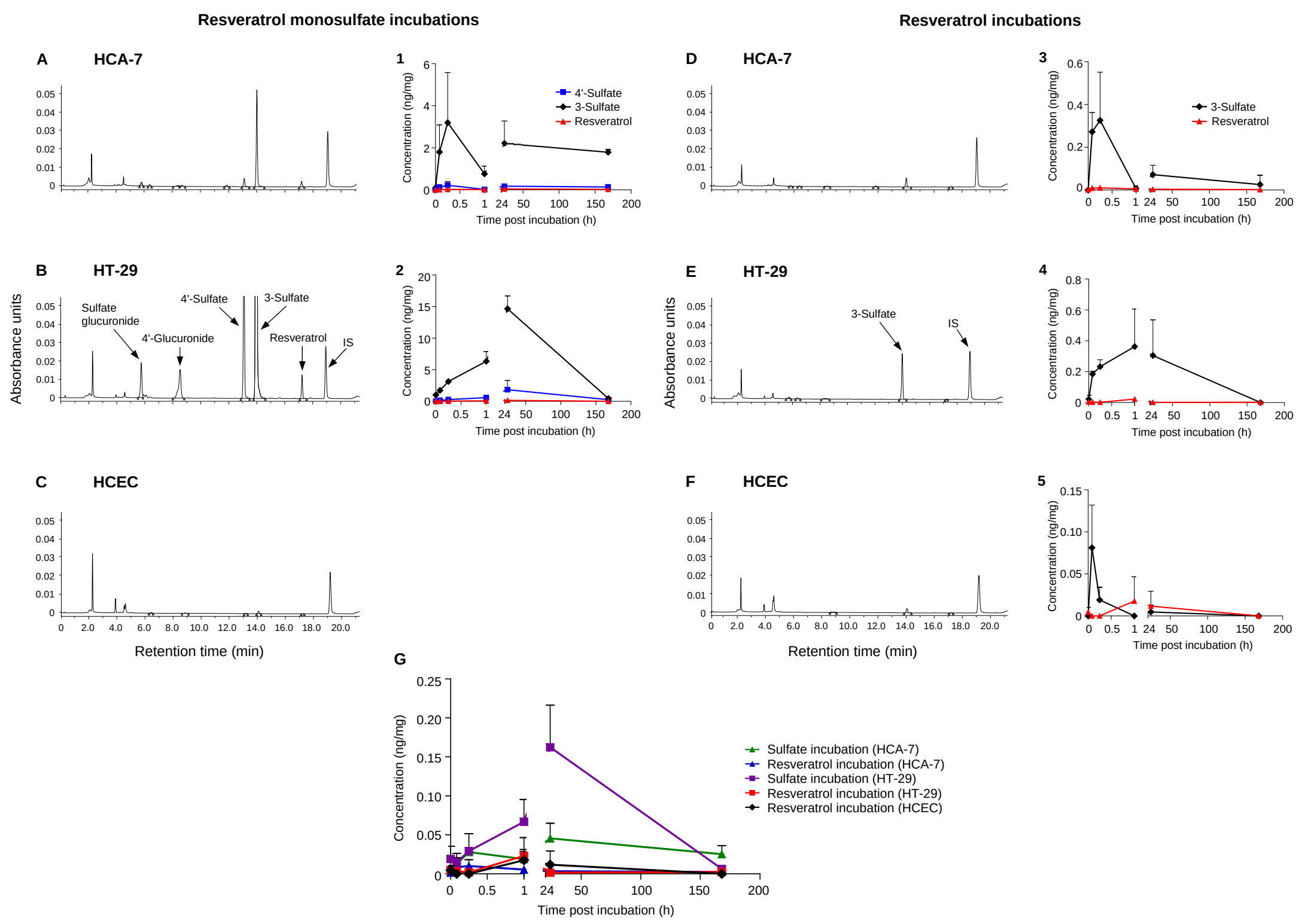
Resveratrol monosulfate incubations
Resveratrol incubations
A
HCA-7
B
HT-29
C
HCEC
D
HCA-7
E
HT-29
F
HCEC
Absorbance units
Sulfate glucuronide
4'-Glucuronide
4'-Sulfate
3-Sulfate
Resveratrol
IS
Retention time (min)
1
2
3
4
5
Concentration (ng/mg)
Time post incubation (h)
4'-Sulfate
3-Sulfate
Resveratrol
G
Sulfate incubation (HCA-7)
Resveratrol incubation (HCA-7)
Sulfate incubation (HT-29)
Resveratrol incubation (HT-29)
Resveratrol incubation (HCEC)

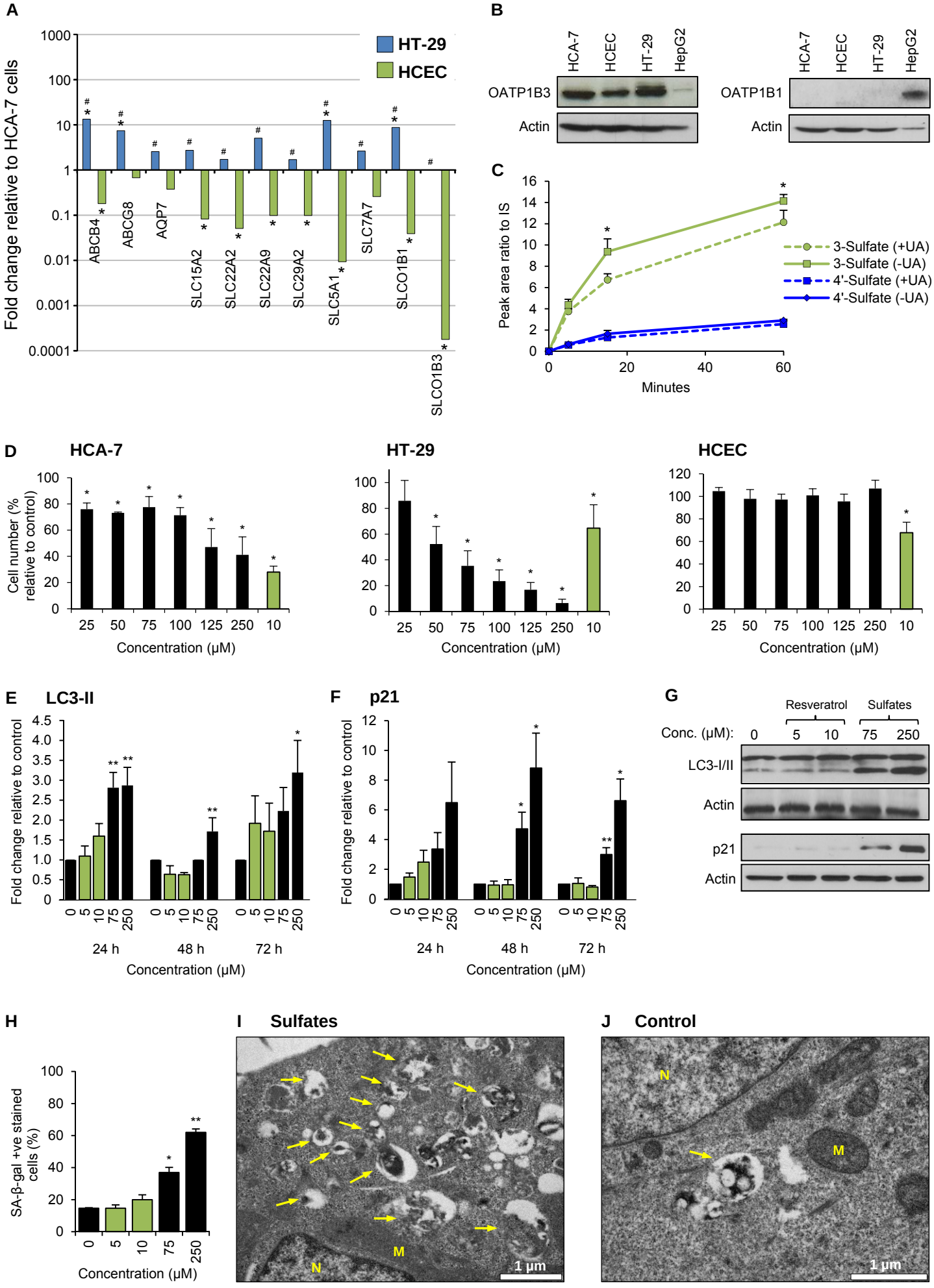
A
HT-29
HCEC
Fold change relative to HCA-7 cells
ABCB4
ABCG8
AQP7
SLC15A2
SLC22A2
SLC22A9
SLC29A2
SLC5A1
SLC7A7
SLCO1B1
SLCO1B3
B
HCA-7
HCEC
HT-29
HepG2
OATP1B3
Actin
OATP1B1
C
Peak area ratio to IS
Minutes
3-Sulfate (+UA)
3-Sulfate (-UA)
4'-Sulfate (+UA)
4'-Sulfate (-UA)
D
HCA-7
HT-29
HCEC
Cell number (% relative to control)
Concentration (μM)
E
LC3-II
Fold change relative to control
24 h
48 h
72 h
Concentration (μM)
F
p21
G
Resveratrol
Sulfates
Conc. (μM):
LC3-I/II
Actin
p21
H
SA-β-gal +ve stained cells (%)
Concentration (μM)
I
Sulfates
N
M
1 μm
J
Control
N
M
1 μm

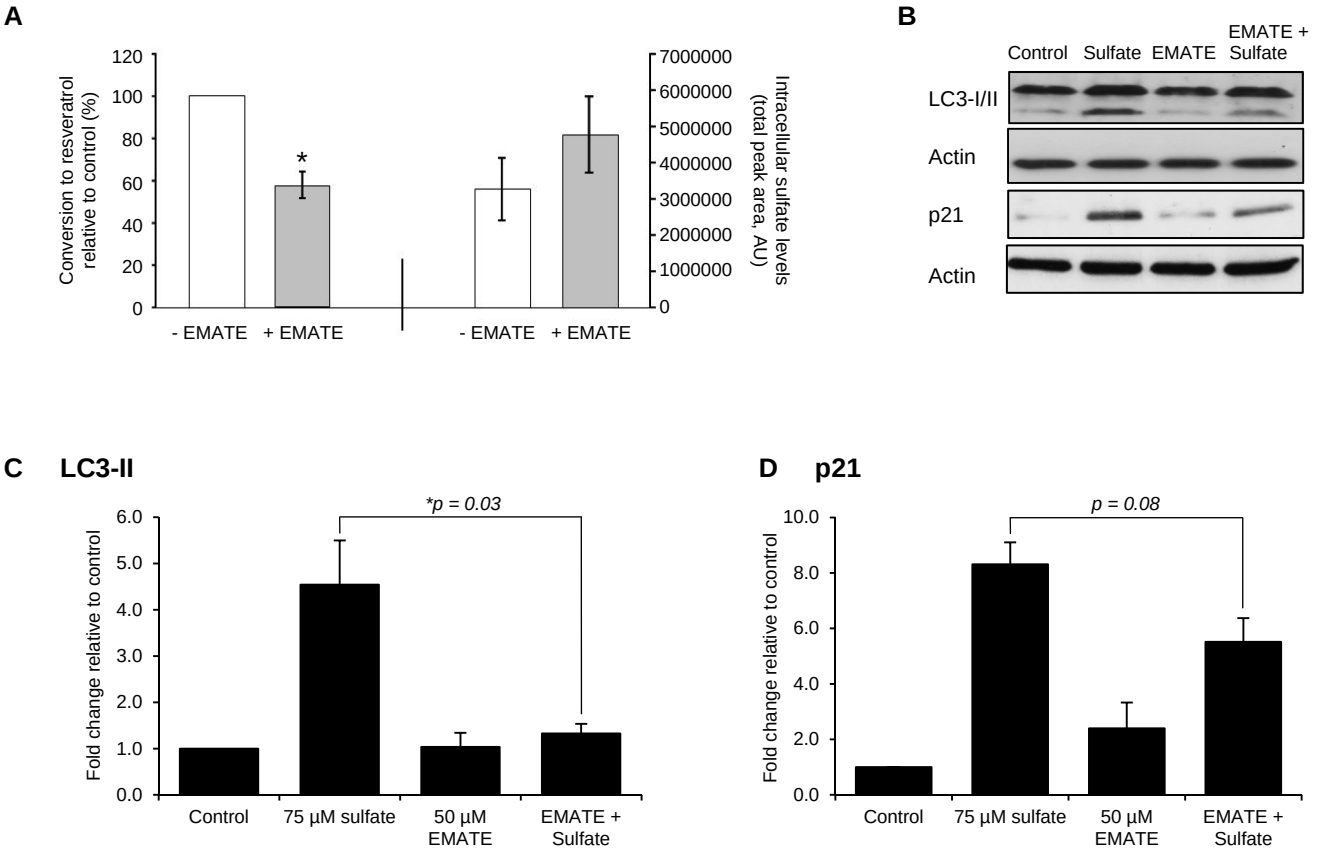
A
Conversion to resveratrol relative to control (%)
120
100
80
60
40
20
0
*
- EMATE
+ EMATE
Intracellular sulfate levels (total peak area, AU)
7000000
6000000
5000000
4000000
3000000
2000000
1000000
0
- EMATE
+ EMATE
B
Control
Sulfate
EMATE
EMATE + Sulfate
LC3-I/II
Actin
p21
Actin
C
LC3-II
*p = 0.03
Fold change relative to control
6.0
5.0
4.0
3.0
2.0
1.0
0.0
Control
75 µM sulfate
50 µM EMATE
EMATE + Sulfate
D
p21
p = 0.08
Fold change relative to control
10.0
8.0
6.0
4.0
2.0
0.0
Control
75 µM sulfate
50 µM EMATE
EMATE + Sulfate

Supplementary Materials and Methods

Metabolite synthesis

Resveratrol was treated with SO_3.DMF and the products isolated using column chromatography to yield a mixture of 3-*O*- and 4′-*O*-resveratrol sulfates (3:2 ratio). Mono-glucuronides of resveratrol were synthesised by differential protection of the phenolic groups of resveratrol followed by addition of glucuronic acid *via* its α-1′-trichloroacetimidate-methyl ester. Deprotection and purification afforded the desired products as individual glucuronide isomers. The powdered sulfate mixture was stored at -80°C; under these conditions it was stable for >2 years, as demonstrated by UV-HPLC analysis.

Clinical trials and pharmacokinetic analysis

Details of the resveratrol clinical trials involving healthy volunteers and patients undergoing colorectal surgery have been described previously (10), (17). These trials were approved by the Nottingham UK Research Ethics Committee and the University of Michigan Institutional Review Board and were conducted in accordance with the applicable guidelines on Good Clinical Practice. Plasma and colorectal mucosa samples were extracted and analysed using a validated HPLC-UV assay (10), (17), (18). Concentrations were estimated based on a resveratrol standard curve or were accurately quantified using standard curves constructed for the individual metabolites. Selected LC-MS/MS analysis was performed to verify metabolite identification using our standard method (18). Pharmacokinetic parameters were modelled using WinNonlin Version 5.3 software (Pharsight Corporation, Mountain View, California, US).

Animal handling and dosing

C57BL/6J adult mice were purchased from Charles River Laboratories. Animals were housed under specific pathogen free conditions and handled in accordance with protocols approved by the Leicester University Ethical Review Panel, under the authority of a UK Home Office Project licence (PPL 80/2167). To define

pharmacokinetics and calculate bioavailability, mice (3 per time point) received a single dose of resveratrol-3-*O*-sulfate and resveratrol-4′-*O*-sulfate (3:2 ratio) by either intravenous injection (6 mg/kg body weight in saline) or intragastrically (120 mg/kg in saline) and were culled at various times post dosing (0, 5, 15, 30, 60 minutes, 2 h, 6 h, 24 h). Plasma concentrations of resveratrol plus all detectable metabolites were quantified and the plasma concentration versus time curves constructed using average levels for 3 mice per time point. Bioavailability of the individual resveratrol sulfates was calculated from the ratio of AUC_{inf} values following oral versus IV administration, taking into account the different doses. In a separate but identical pharmacokinetic study, resveratrol was administered intragastrically (120 mg/kg). In both studies the small intestines and colon were flushed with PBS and the mucosa obtained by gentle scraping. Tissues and plasma were snap frozen in liquid nitrogen and stored at -80°C prior to HPLC-UV analysis using the same methods employed for human samples.

Cell culture

HT-29 and HCA7 cells authenticated by microsatellite genotyping were newly obtained from the Health Protection Agency (HPA) culture collections (Sailsbury, UK). HCEC cells were from the Nestle Research Centre (Lausanne, Switzerland). Cell numbers were determined using a Z2 Coulter Particle Count and Size Analyser (Beckman Coulter, High Wycombe, UK). Cell cycle analysis was performed by flow cytometry (FACS Aria II, BD Bioscience) using ModFit LT software (Version 3.2), with propidium iodide staining. The extent of necrosis and apoptosis was measured by flow cytometry using an Annexin V-FITC assay (Bender MedSystems, GmbH, Vienna, Austria) and the latter was confirmed by cleaved caspase-3 analysis. Antibodies used to assess protein levels in cell lysates were as follows: LC3 A/B (Cell Signalling Tech. #4108), p21 Waf1/Cip1 (Cell Signalling Tech. #2947), OATP1B1 (Abcam #ab103065), OATP1B3 (Abcam #ab139120) and actin (Santa Cruz Biotechnologies #sc-1616). For senescence-associated β-galactosidase assay, HT29 cells were plated ($1.3x10^5$ cells/well) in 6-well plates and treated with resveratrol or resveratrol sulfates for 72 h. Cells were stained using a senescence β-galactosidase staining kit (Cell Signalling Tech. #9860) according to the manufacturer's instructions and viewed under a Nikon Eclipse TE2000 inverted microscope (200x total

magnification). The percentage of SA-β-galactosidase positive stained cells was determined by counting the number of blue cells of the total cell number in several fields of view in three independent experiments.

QRT-PCR analysis

Total RNA was extracted from the cell pellets using an RNeasy Mini kit (Qiagen) including on-column DNase digestion. Reverse transcription was performed using the RT^2 First Strand Kit (Qiagen) with 1 µg of RNA per sample. Gene expression was analysed for each cell type in triplicate using the RT^2 Profiler PCR Array - Human Drug Transporters (Qiagen) according to the manufacturer's instructions.

Reactions were run on a Step One Plus thermal cycler (Applied Biosystems) with an initial activation step at 95°C for 20 seconds followed by 40 cycles of 95°C for 15 seconds and 60°C for 1 minute. Raw data were analysed with Step One v2.2 software and Microsoft Excel. To assess gene expression, the ΔCt was determined (Ct minus average Ct value of the housekeeping genes for each plate array) and was used to calculate the ΔΔCt (ΔCt value of the target gene minus ΔCt value of the reference gene) for each cell line. Fold change was calculated as $2^{-\Delta\Delta Ct}$.

Analysis of cell pellets to determine intracellular resveratrol and metabolite concentrations:

After treatments, cells (~10 million) were washed (PBS), trypsinised, then accurately counted prior to pelleting and freeze-thawing, using three cycles of liquid nitrogen followed by 50°C water (1 min). Resveratrol species were extracted using acetone combined with sonication and the supernatant was concentrated to dryness under N_2. Samples were reconstituted in MeOH: H_2O (50: 50) and analysed by HPLC-UV using the method described above. Calibration curves were constructed using cell pellets spiked with resveratrol and monosulfates to allow quantitation of intracellular concentrations. Measured intracellular concentrations were normalised according to cell numbers and converted to ng/mg cells.

Ursolic acid incubations

HT-29 cells were pre-incubated with ursolic acid (20 μM in DMSO) or DMSO alone (control) for 10 min prior to adding a 3:2 mixture of resveratrol-3-*O*- and -4′-*O*-sulfate (75 μM). Incubations were stopped 5, 15 or 60 min after addition of resveratrol sulfates and processed as described above then the extracts were analysed by UV-HPLC. Measured intracellular concentrations were normalised using an internal standard (naringenin) and corrected for cell number. Experiments were performed in triplicate.

EMATE incubations

HT-29 cells were incubated with EMATE (50 μM) for 1 h, after which resveratrol sulfates (75 μM of 3-*O*- and 4′-*O*-sulfate, 3:2 mixture) were added, and incubations terminated 24 h later. Generation of resveratrol in cell pellets was determined by HPLC-UV analysis as described above. A positive control experiment was also performed using [6,7-^{3}H]-estrone sulfate (42 pmol, 5 x 10^{6} DPM, American Radiolabeled Chemicals Inc.) as a substrate, to independently demonstrate that EMATE effectively inhibits steroid sulfatase in HT-29 cells, at the concentration employed. Conversion of estrone sulfate to estrone was determined according to an established method (26) by toluene extraction of media (2 mL), using [^{14}C]-resveratrol to correct for procedural losses, and radioactivity was measured by liquid scintillation counting. Using this protocol EMATE significantly reduced the enzymatic hydrolysis of estrone sulfate to estrone by 30%, compared to control incubations without EMATE.

Transmission electron microscopy

HT-29 cells were treated with 250 μM resveratrol sulfates or DMSO vehicle (0.1%) for 72 h. Cells were harvested, fixed (2% glutaraldehyde in 0.1M sodium cacodylate buffer, pH 7.4, followed by 1.0% osmium tetroxide and 0.5% aqueous uranyl acetate) and dehydrated using an ethanol series before embedding in low viscosity resin. Electron microscopy of random sections was performed using a JEOL JEM-1400 Transmission Electron Microscope (JEOL UK Ltd., Welwyn Garden City), at 80 kV, on ultrathin sections (90 nm) contrasted with 2% aqueous uranyl acetate and lead citrate. Images were captured using an Olympus SIS Megaview III digital camera with iTEM software.

A **Resveratrol**

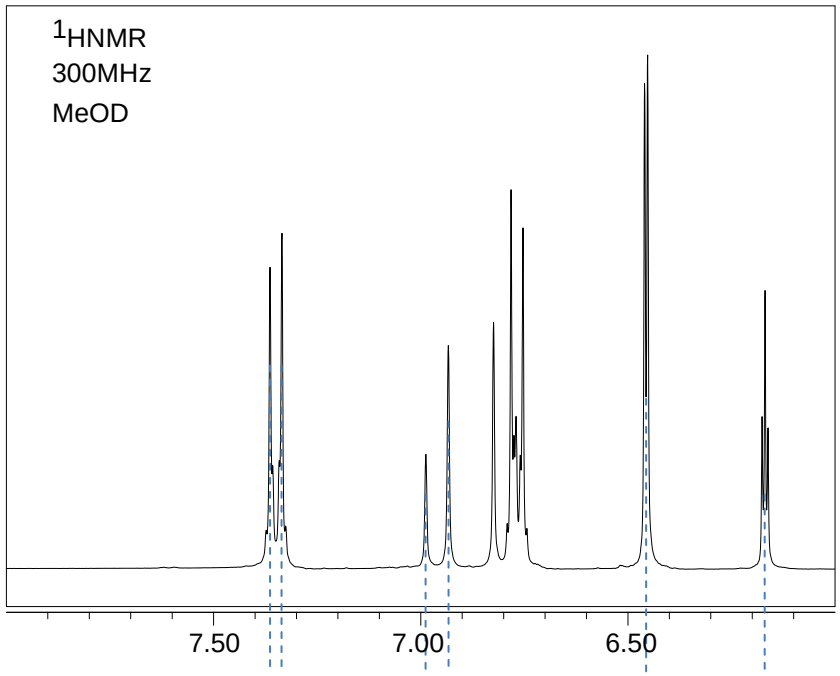

B **Resveratrol monosulfate mixture used in *in vitro* and *in vivo* studies**

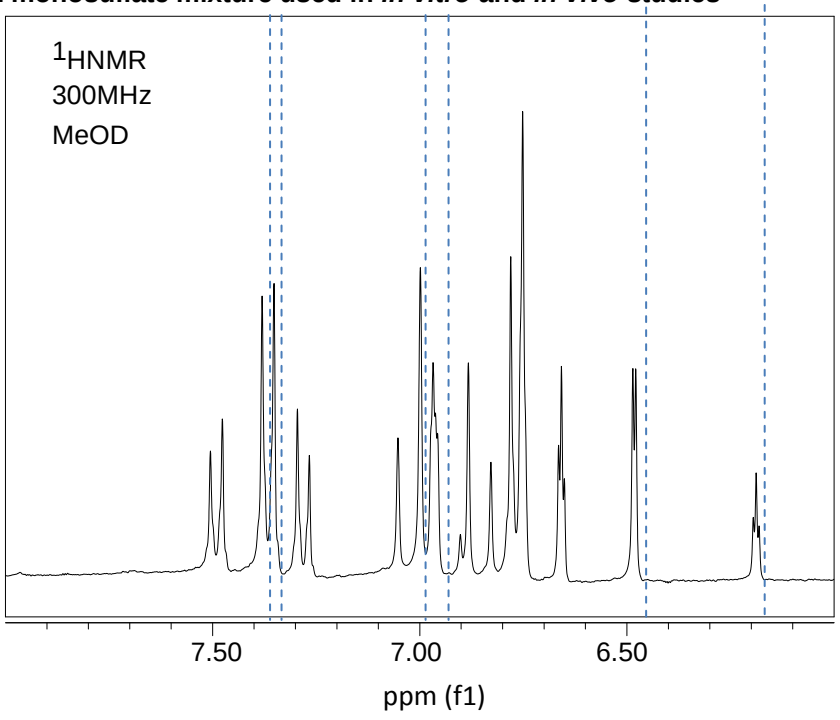

Figure S1: ^{1}H-NMR spectrum of resveratrol sulfate. ^{1}H-NMR spectra of resveratrol (**A**) and resveratrol monosulfates (**B**). Dashed lines indicate where peaks originating from resveratrol would appear if present in the sulfate mixture.

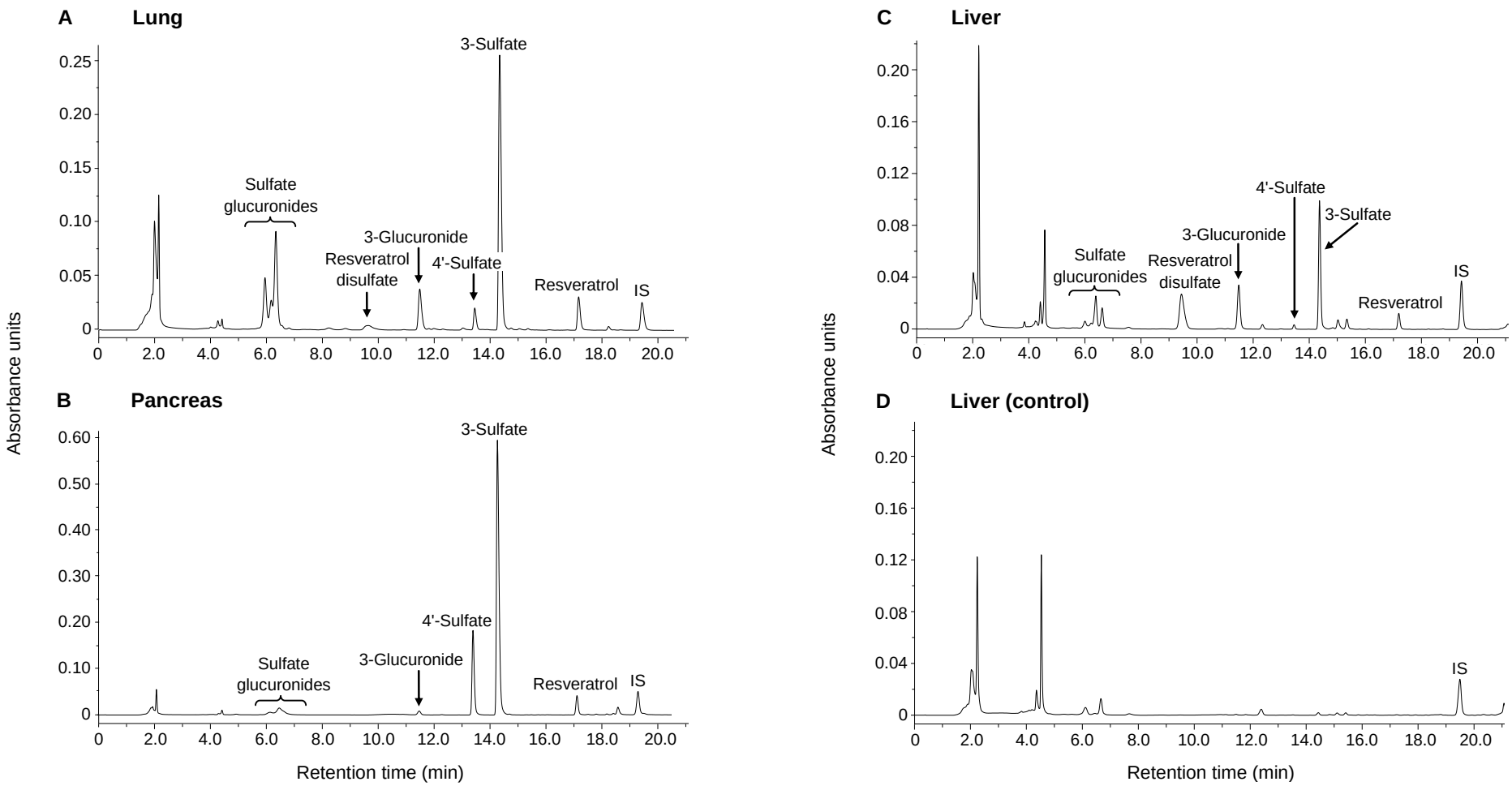

Figure S2: Metabolite profile in mouse tissues after oral resveratrol sulfate. Representative HPLC-UV chromatograms of extracts of lung (**A**), pancreas (**B**) and liver (**C**) taken 0.5 h post-dosing from mice that received 120 mg/kg resveratrol sulfates intragastrically (3:2 mixture of resveratrol-3-*O*- and -4'-*O*-sulfate). Liver (control) (**D**) is from a mouse that received saline vehicle. Metabolites detected were resveratrol sulfate glucuronide isomers, resveratrol disulfate (only in the lung), resveratrol-3-*O*-glucuronide, resveratrol-4'-*O*-sulfate, resveratrol-3-*O*-sulfate and resveratrol.

Metabolites were identified by comparison of retention times with synthetic standards, where available, and confirmed by LC-MS/MS. Peak designated as IS corresponds to the internal standard, naringenin.

A **Plasma**

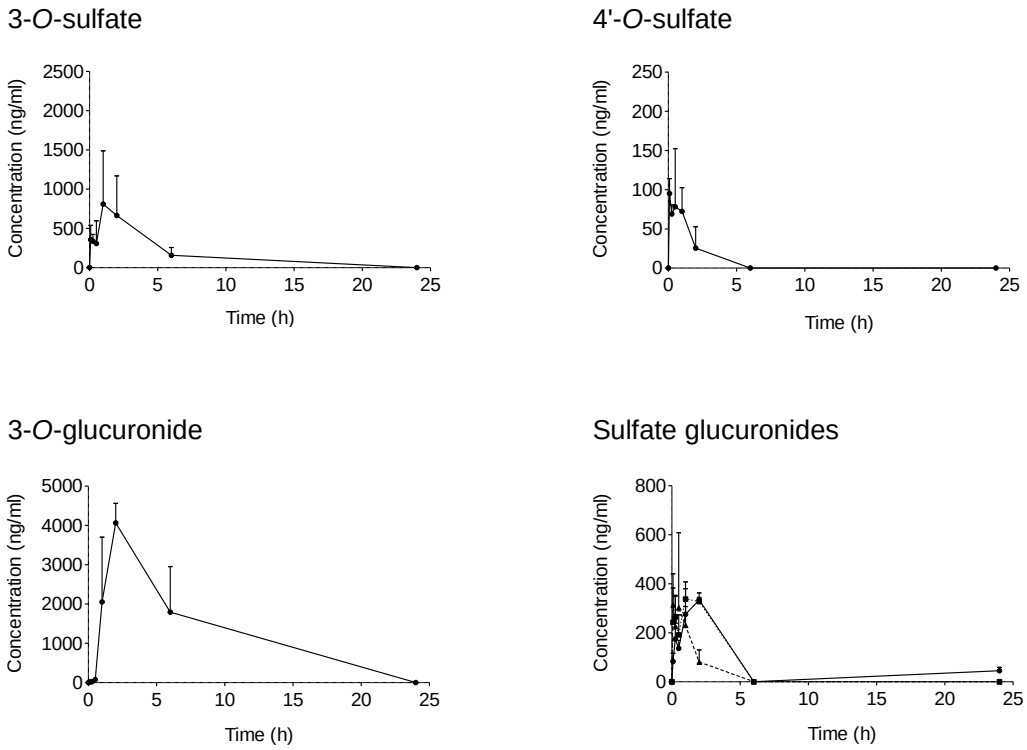

B **Mucosa**

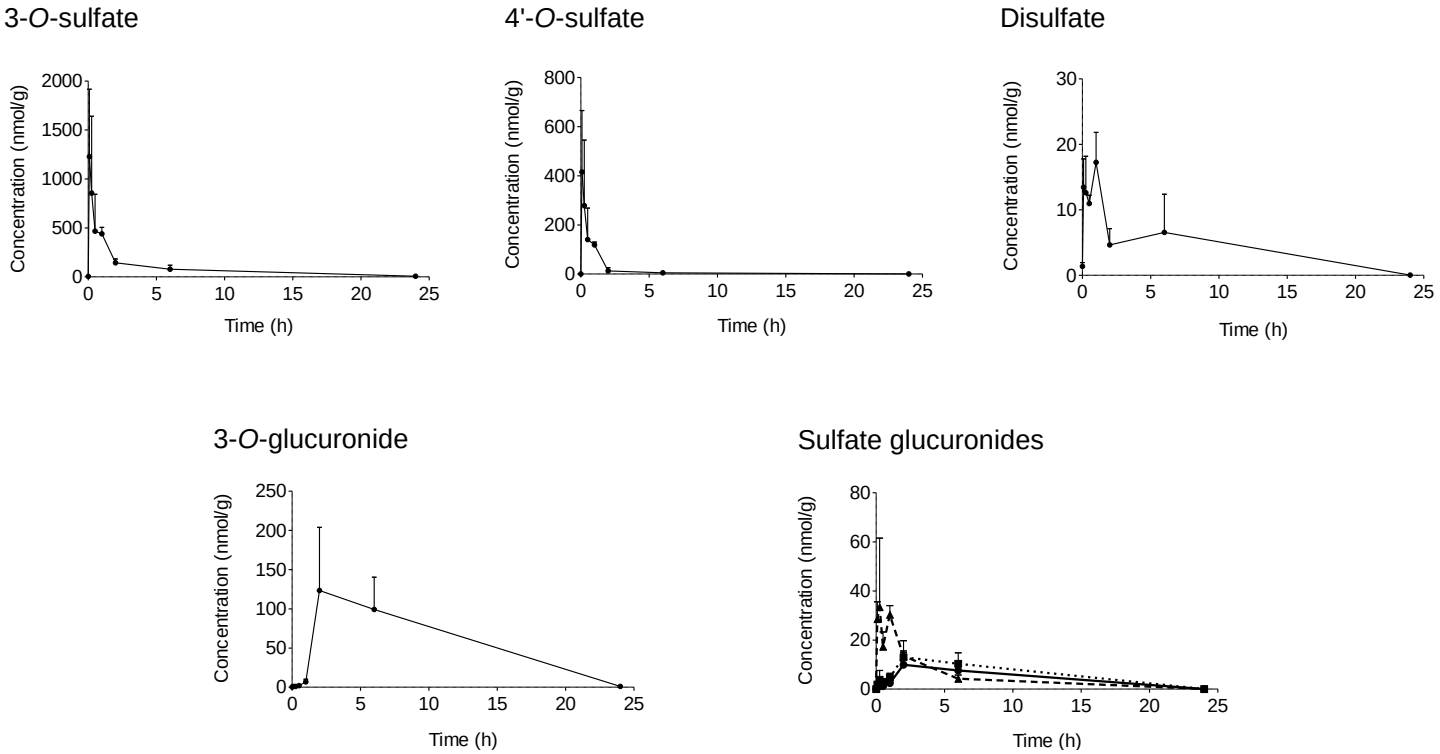

Figure S3: **Metabolite pharmacokinetics in mice.** Concentrations of resveratrol metabolites in mouse plasma

and mucosa over 24 h following intragastric administration of 120 mg/kg resveratrol sulfates (3:2 mixture of resveratrol-3-*O*- and -4'-*O*-sulfate). Concentrations were determined by HPLC-UV analysis of plasma/tissue extracts. Values for each point are the mean + SD of three mice. As an indicator of variability, the coefficient of variation for plasma concentrations of resveratrol-4'-*O*-sulfate ranged from 17% (15 min) to 106% (120 min) after gavage dosing, and from 27% (15 min) to 101% (60 min) for resveratrol-3-*O*-sulfate.

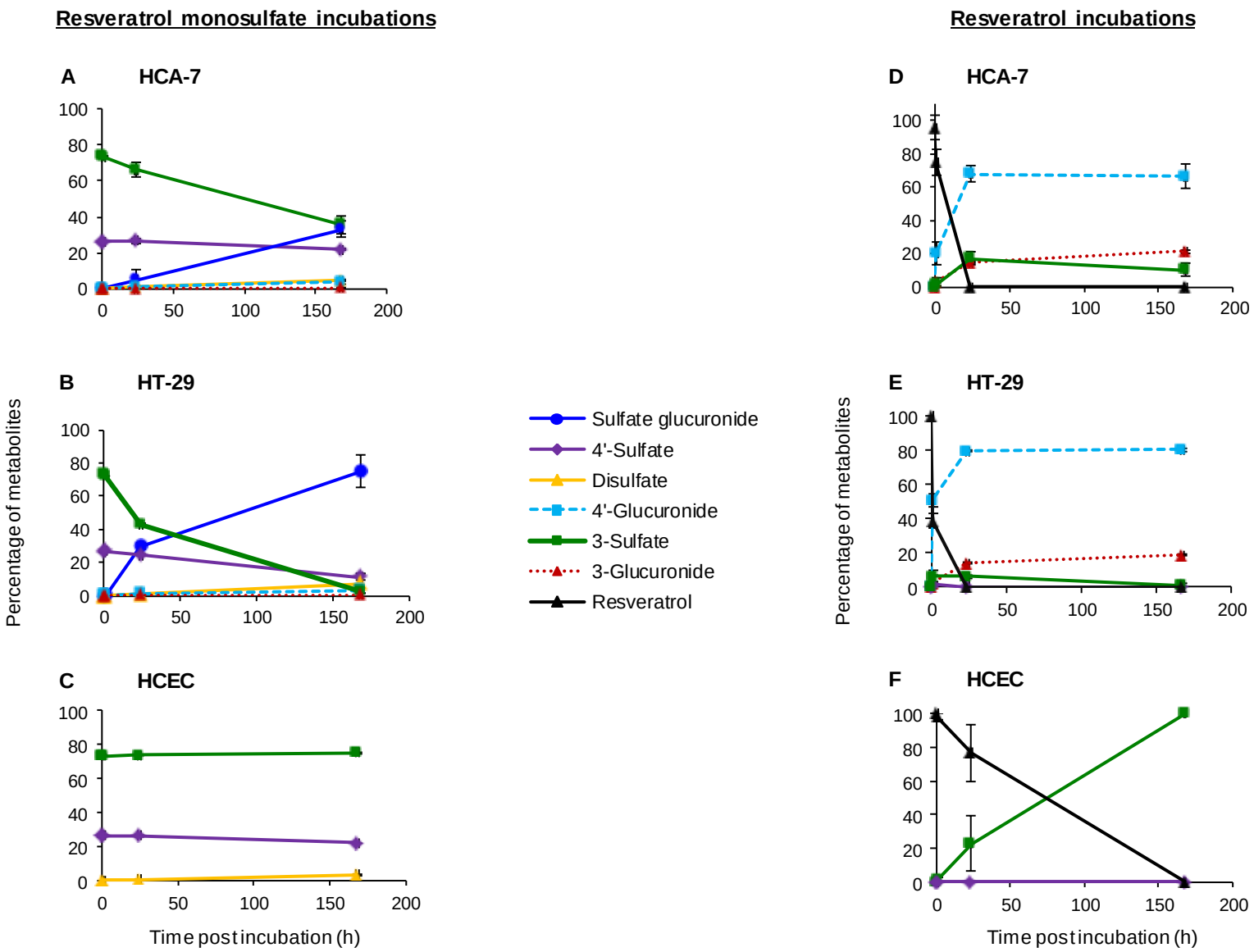

Figure S4: **Kinetics of resveratrol/metabolite formation in cell media.** Resveratrol and its metabolites detected in conditioned media of HCA-7 (**A**), HT-29 (**B**) and HCEC (**C**) cells incubated with a 3:2 mixture of resveratrol-3-*O*-sulfate and resveratrol-4'-*O*-sulfate (75 µM) over seven days,

expressed as percentage of total resveratrol species per time point. Resveratrol species detected in conditioned media of HCA-7 (**D**), HT-29 (**E**) and HCEC (**F**) cells incubated with 10 μM resveratrol over seven days, expressed as percentage of total resveratrol species per time point. Data are the mean ± SD of three independent experiments.

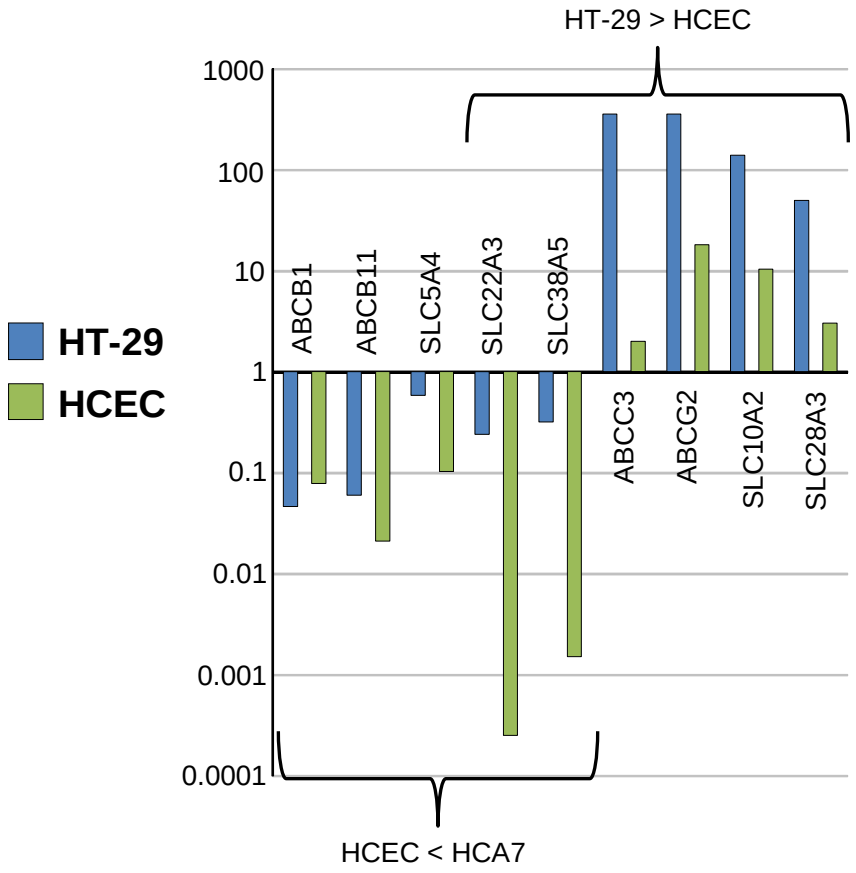

Figure S5: Expression of transporter genes. Comparison of the basal expression of drug transporter genes in HCA-7, HT-29 and HCEC cells determined using an RT^2 Profiler PCR array. Chart shows only those genes where expression is significantly higher in either HT-29 or HCA-7 compared to HCEC cells. However, genes where the rank order of expression is HT-29 > HCA-7 > HCEC are excluded, since these are shown in Figure 5A. Experiments were conducted in triplicate and data expressed relative to levels in HCA-7 cells (set as 1.0). Only genes for which significant differences ($p < 0.01$, Two-Way ANOVA) were detected in ΔCt value between at least one of the possible pairings are illustrated.

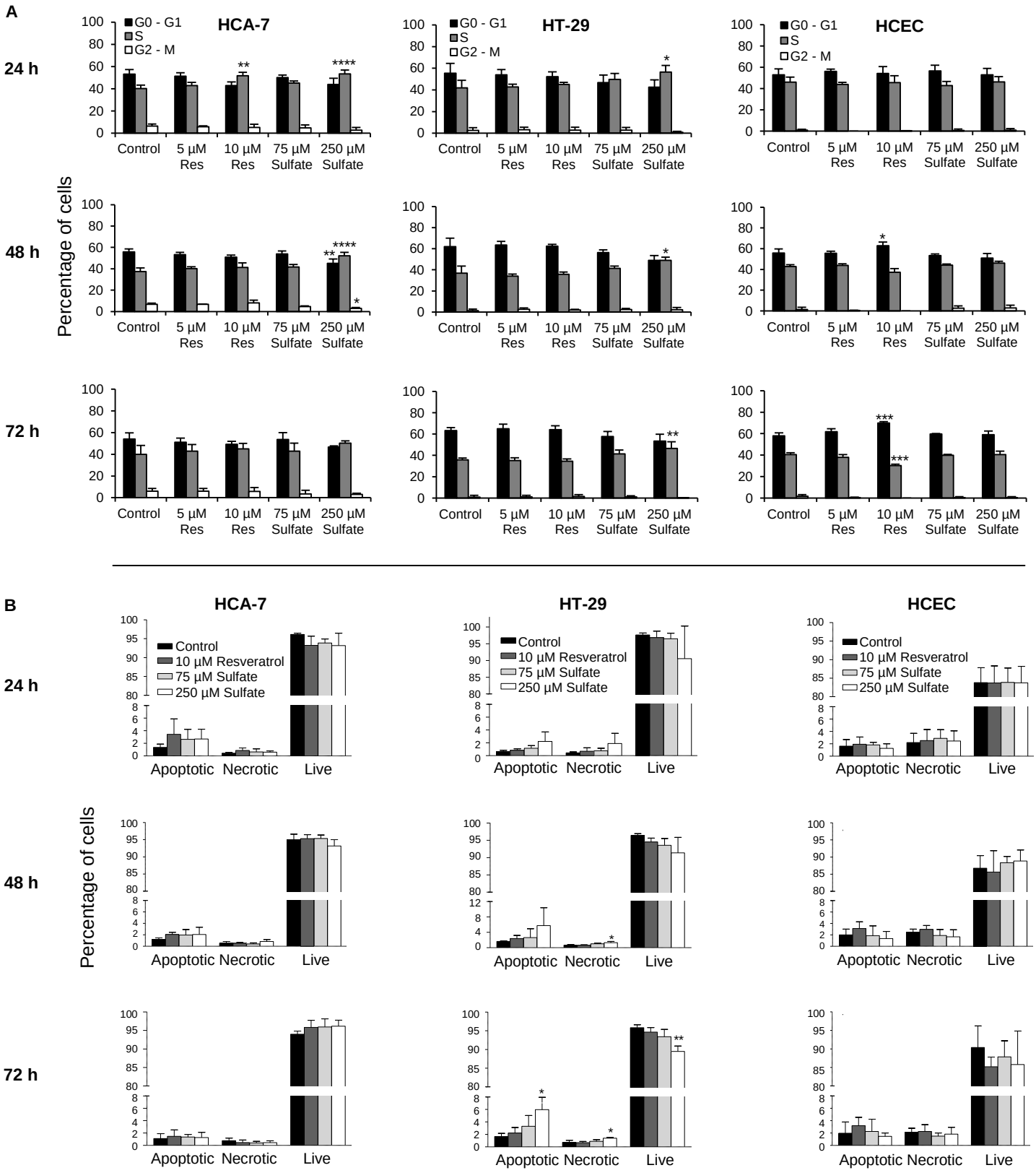

Figure S6: Cell cycle and apoptosis analysis. Percentage of colon cells in each stage of the cell cycle at 24, 48 and 72 h post-treatment with 5 and 10 µM of resveratrol and 75 and 250 µM of resveratrol monosulfates (**A**). Asterisks indicate level of significance following One-Way ANOVA analysis (*$p \leq 0.05$, **$p \leq 0.01$, ***$p \leq$

*0.02, ****$p \leq 0.002$).* Percentage of apoptotic, necrotic and live colon cells at 24, 48 and 72 h post-treatment with 10 µM of resveratrol and 75 and 250 µM of resveratrol monosulfates (**B**). Asterisks indicate level of significance following One-Way ANOVA analysis (*$p \leq 0.05$, **$p \leq 0.005$). Note the break in the y-axis.

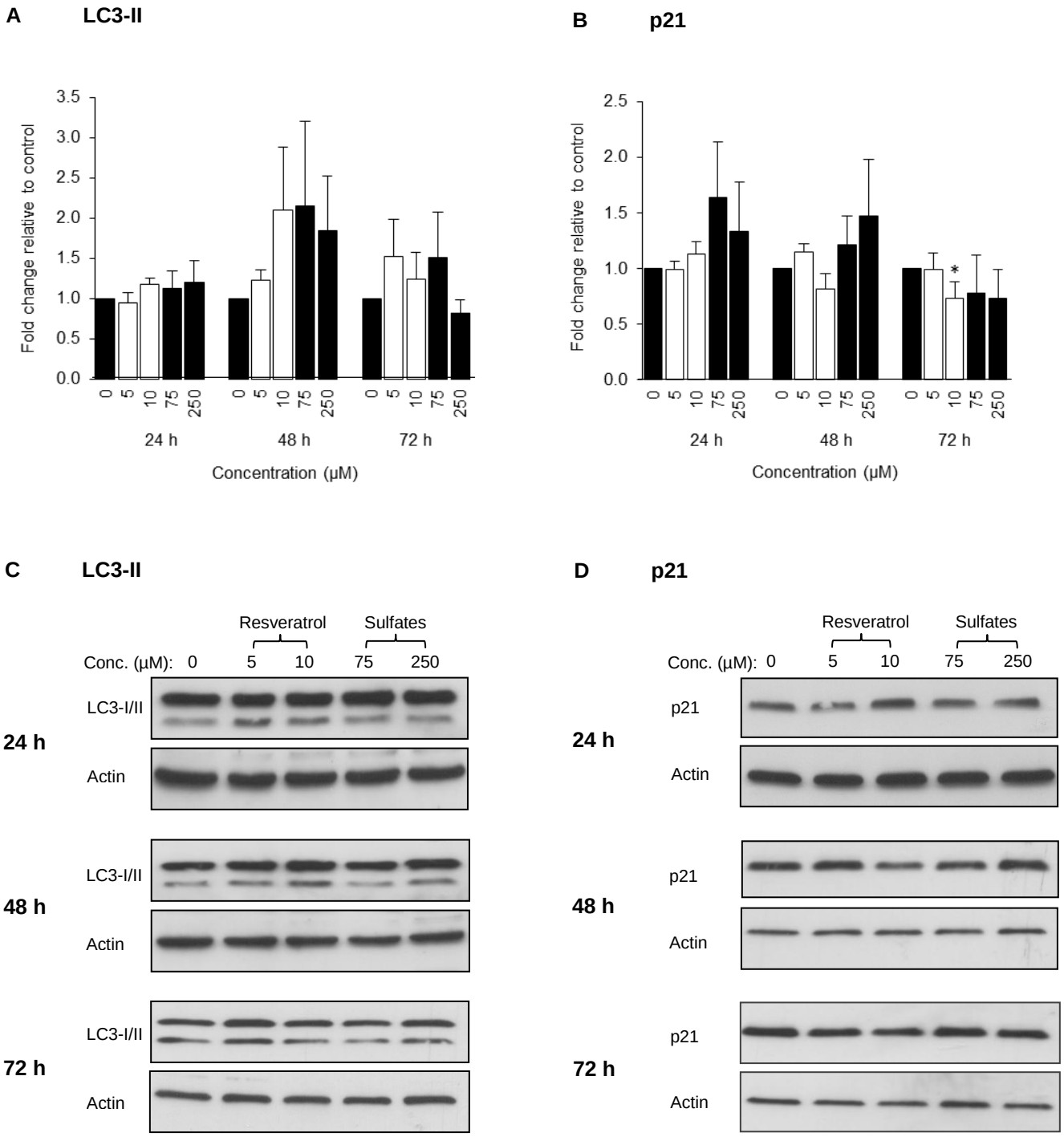

Figure S7: Autophagy and senescence markers in HCEC cells. Levels of LC3-II (**A**) and p21 (**B**) relative to solvent control, following incubation of HCEC cells with resveratrol (clear bars), or a mixture of 75 µM resveratrol-3-*O*-sulfate and resveratrol-4'-*O*-sulfate (3: 2) (black bars) for 24, 48 and 72 h. Values are the mean + SEM of three independent experiments. A significant reduction compared to control is indicated by $*p \leq 0.05$ (Student's t-test). Representative Western blots showing the expression of LC3-I/II (**C**) and p21 (**D**) proteins in HCEC cells incubated with resveratrol or resveratrol sulfate mixture for up to 72 h.

Table S1

A

	Average plasma C_{max} (resveratrol standard curves, μM)					Average plasma C_{max} (authentic standard curves, μM)			
	4′-Gluc	**3-Gluc**	**4′-Sulfate**	**3-Sulfate**	**Resveratrol**	**4′-Gluc**	**3-Gluc**	**4′-Sulfate**	**3-Sulfate**
0.5 g	0.56 ± 0.20 (0.4 – 0.7)	0.67 ± 0.55 (0.3 – 1.3)	0.10 ± 0.01 (0.10 – 0.11)	0.89 ± 0.17 (0.8 – 1.1)	0.61 ± 0.26 (0.4 – 0.9)	1.5 ± 0.53 (1.0 – 2.1)	1.8 ± 1.5 (0.9 – 3.5)	0.2 ± 0.02 (0.2 – 0.3)	2.8 ± 0.52 (2.4 – 3.4)
1.0 g	2.5 ± 1.6 (1.1 – 4.2)	1.4 ± 0.56 (0.8 – 1.7)	0.28 ± 0.07 (0.2 – 0.4)	4.7 ± 0.86 (4.0 – 5.6)	0.48 ± 0.14 (0.3 – 0.6)	5.8 ± 3.7 (2.6 – 9.8)	3.3 ± 1.3 (1.8 – 4.2)	0.4 ± 0.18 (0.2 – 0.6)	11.5 ± 2.1 (9.8 – 13.8)
2.5 g	3.4 ± 2.1 (2.1 – 5.8)	3.7 ± 3.6 (1.2 – 7.7)	0.01 ± 0.01 (0 – 0.02)	4.2 ± 1.00 (3.3 – 5.3)	1.9 ± 1.1 (0.6 – 2.6)	8.4 ± 5.1 (5.3 – 14.3)	9.1 ± 8.8 (2.9 – 19.2)	0.1 ± 0.05 (0 – 0.1)	11.1 ± 2.6 (8.6 – 13.8)
5.0 g	4.5 ± 0.73 (3.7 – 5.0)	8.2 ± 3.0 (5.1 – 11.1)	0.42 ± 0.05 (0.4 – 0.5)	6.8 ± 2.5 (4.8 – 9.5)	5.4 ± 2.6 (2.3 – 7.0)	13.5 ± 2.2 (10.9 – 14.8)	24.6 ± 9.2 (15.3 – 33.6)	0.7 ± 0.23 (0.5 – 1.0)	23.2 ± 8.8 (16.0 – 33.1)

B

		Estimated plasma concentration (μM)
1.0 g	**Resveratrol-3-*O*-sulfate**	21.5 ± 7.6 (8.4 – 31.7)
	Resveratrol-4'-*O*-glucuronide	8.3 ± 4.8 (3.8 – 17.8)
	Resveratrol-3-*O*-glucuronide	6.8 ± 3.3 (1.8 – 12.3)

Table S1: **Levels of resveratrol and metabolites in human plasma.** (**A**) Concentration of resveratrol and its metabolites in human plasma estimated using resveratrol as standard or accurately measured using metabolite standards. Healthy volunteers received resveratrol at a dose of 0.5, 1.0, 2.5 or 5.0 g daily for 29 days. Concentrations were determined by HPLC-UV analysis of plasma taken on a day during the last week of intervention. Values are the mean ± SD maximum plasma concentrations (C_{max}) for 3 randomly selected individuals per dose group. The fold-difference between the estimated and accurate concentrations was calculated and this correction factor was then used to estimate the mean plasma C_{max} and range for the entire group that received 1g resveratrol (10 volunteers), to give a better indication of the relevant concentration range achievable in humans; these data are shown in Table B. (**B**) Estimated concentration of resveratrol metabolites in plasma of healthy volunteers following 1.0 g resveratrol dosing for 29 days, based on metabolite standard curves. Values are the mean ± SD for 10 individuals per dose group. Values in brackets indicate the range of concentrations across the group.

Table S2

A

		Concentration (nmol/g tissue)		
		Left	Right	Overall
0.5 g	Resveratrol-3-*O*-glucuronide	0.13 (0 – 1.22)	52.9 (0 – 506.7)	16.0
	Resveratrol-4'-*O*-glucuronide	0.29 (0 – 1.58)	4.9 (0 – 45.1)	1.7
	Resveratrol-3-*O*-sulfate	1.0 (0 – 6.1)	29.3 (0.35 – 268.7)	9.5
	Resveratrol-4'-*O*-sulfate	0.11 (0 – 0.79)	0.92 (0 – 8.2)	0.35
	Resveratrol sulfate glucuronide	26.4 (0 – 192.9)	34.1 (0 – 237.7)	28.7
	Resveratrol disulfate	1.9 (0 – 21.7)	8.6 (0 – 54.7)	3.9
1.0 g	Resveratrol-3-*O*-glucuronide	0.25 (0 – 0.97)	7.6 (0 – 81.3)	3.6
	Resveratrol-4'-*O*-glucuronide	0.64 (0 – 2.16)	2.0 (0 – 8.5)	1.3
	Resveratrol-3-*O*-sulfate	0.87 (0 – 5.7)	53.8 (2.4 – 638)	24.9
	Resveratrol-4'-*O*-sulfate	0.02 (0 – 0.44)	3.7 (0 – 26.7)	1.7
	Resveratrol sulfate glucuronide	32.9 (7.3 – 82.8)	39.4 (15.3 – 151.3)	35.9
	Resveratrol disulfate	0	0.44 (0 – 5.9)	0.2

B

		Concentration (nmol/g tissue)		
		Left	Right	Overall
0.5 g	Resveratrol-3-*O*-sulfate	0.78 (0 – 1.9)	14.4 (0.67 – 127.7)	4.9
	Resveratrol-4'-*O*-sulfate	0.07 (0 – 1.0)	0.57 (0 – 4.5)	0.2
1.0 g	Resveratrol-3-*O*-sulfate	0.65 (0 – 3.6)	30.2 (1.6 – 366.6)	14.1
	Resveratrol-4'-*O*-sulfate	0.01 (0 – 0.34)	2.4 (0 – 12.6)	1.1

C

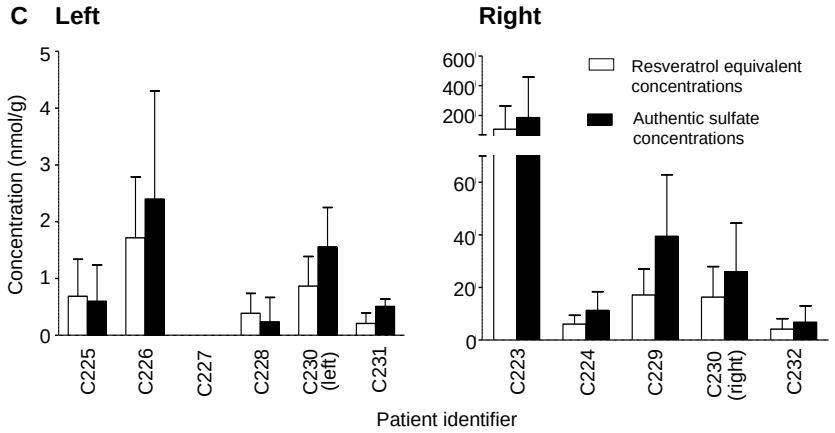

Table S2: Comparison of accurately quantified and estimated colorectal tissue levels of resveratrol metabolites. Accurately quantified (**A**) and estimated (**B**) colorectal tissue levels of resveratrol metabolites in cancer patients following 0.5 and 1.0 g resveratrol daily for 8 days. Values are the mean of concentrations (nmol/g tissue) in 10 patients per dose group. On the 0.5 g dose, 7 patients presented with left-sided tumours and 3 with right-sided tumours. On the 1.0 g dose, 6 patients presented with left-sided tumours and 5 with right-sided tumours (one patient had synchronous left and right-sided tumours). Values in brackets indicate the range of concentrations determined across different tissues (proximal and distal to tumour)

in all patients. (**A**) Accurate quantitation of monosulfate concentrations in all patient samples was calculated using resveratrol-3-*O*-sulfate and resveratrol-4'-*O*-sulfate standard curves. Glucuronide concentrations were estimated based on extraction of selected patient samples (3 patients per dose) with resveratrol-4'-*O*-glucuronide standards, whereas resveratrol disulfate and resveratrol sulfate glucuronide concentrations were based on resveratrol sulfate and resveratrol-4'-*O*-glucuronide standard curves respectively. (**B**) Shows the average resveratrol-3-*O*-sulfate and resveratrol-4'-*O*-sulfate concentrations in samples from the same patients calculated as resveratrol equivalents, using resveratrol standard curves. Individual patient data are shown in (**C**) to graphically illustrate the difference between the accurate and estimated concentrations of resveratrol-3-*O*-sulfate in non-malignant and tumour tissue removed from the colon of patients that received the 1.0 g resveratrol dose. Concentrations are presented as resveratrol equivalents (clear bars) and as authentic resveratrol-3-*O*-sulfate concentrations (black bars) from patients with left-sided tumours (left graph) or right-sided tumours (right graph). Values are the mean of 3 to 7 sections of colon tissue (including tumour tissue) per patient. A break in the y-axis has been incorporated for clarity.

A Resveratrol-3-*O*-sulfate

	T_{max} (h)		C_{max} (nmol/g)		T_{last} (h); C_{last} (nmol/g)		AUC_{all} (nmol/g/h)	
	IV	IG	IV	IG	IV	IG	IV	IG
Plasma	0.083	1	13.8	2.6	24; 0.04	24; 1.0	1,295	4,250
Liver	0.083	2	58.8	34.3	6; 1.7	6; 29.9	60.6	438
Lung	0.083	0.083	4.3	39.6	2; 0.1	6; 0.6	1.3	27.2
Mucosa	0.5	0.083	66.0	1,224	6; 8.7	24; 1.2	168	1,989
Pancreas	0.083	0.5	3.1	47.7	0.5; 0.15	6; 0.6	0.49	32.4

B Resveratrol-4'-*O*-sulfate

	T_{max} (h)		C_{max} (nmol/g)		T_{last} (h); C_{last} (nmol/g)		AUC_{all} (nmol/g/h)	
	IV	IG	IV	IG	IV	IG	IV	IG
Plasma	0.083	0.083	3.3	0.3	2; 0.01	2; 0.08	266	174
Liver	0.083	0.083	1.1	2.1	2; 0.1	2; 0.4	1.04	2.4
Lung	0.083	0.083	0.6	12.4	0.5; 0.2	6; 0.03	0.19	2.6
Mucosa	0.25	0.083	1.9	415	2; 0.3	24; 0.2	3.10	341
Pancreas	0.083	0.5	0.3	12.7	0.5; 0.04	2; 0.1	0.04	7.9

C Resveratrol

	T_{max} (h)		C_{max} (nmol/g)		T_{last} (h); C_{last} (nmol/g)		AUC_{all} (nmol/g/h)	
	IV	IG	IV	IG	IV	IG	IV	IG
Plasma	6	1	0.06	0.6	6; 0.06	6; 0.13	N/A	765
Liver	0.083	2	3.2	2.6	6; 0.1	6; 2.3	3.8	34
Lung	0.083	0.5	0.32	2.2	0.083; 0.32	2; 0.1	N/A	1.1
Mucosa	0.25	0.25	1.5	14.8	6; 0.34	24; 0.2	5.69	81
Pancreas	0.083	0.5	0.31	1.8	0.083; 0.31	2; 0.2	N/A	1.6

Table S3: Mouse pharmacokinetic parameters following resveratrol sulfate administration. Pharmacokinetic parameters for resveratrol-3-*O*-sulfate (**A**), resveratrol-4'-*O*-sulfate (**B**) and resveratrol (**C**) in mouse plasma and tissues following intravenous and intragastric dosing of resveratrol sulfates at 6 mg/kg and 120 mg/kg respectively. Parameters were calculated on an average of 3 tissues per group using WinNonlin software. Plasma concentrations for C_{max} and C_{last} are expressed in µM and ng/h/ml for AUC_{all}. Tissue

concentrations are given in nmol/g, which are equivalent to µM values. C_{last} indicates the last quantifiable concentration in the different matrices. N/A indicates where it was not possible to calculate the AUC_{all} for resveratrol in plasma, lung and pancreas following IV dosing of resveratrol sulfates.

A

		Plasma AUC_{all} (nmol/g/h)							
		3-*O*-sulfate	**4'-*O*-sulfate**	**3-*O*-glucuronide**	**Sulfate-glucuronide 1**	**Sulfate glucuronide 2**	**Sulfate glucuronide 3**	**Resveratrol**	**Total AUC**
Sulfate dosing	**AUC_{all}**	4250	174	31464	1141	1229	574	762	**39594**
	% of total	*10.7*	*0.4*	*79.5*	*2.9*	*3.1*	*1.4*	*1.9*	***100***
Resveratrol dosing	**AUC_{all}**	16644	-	108530	15301	11226	-	6980	**158681**
	% of total	*10.5*	*-*	*68.4*	*9.6*	*7.1*	*-*	*4.4*	***100***

B

	Plasma half-life (h)		
	3-*O*-Sulfate	**4'-*O*-Sulfate**	**Resveratrol**
Resveratrol dosing	3.2	-	11.0
Sulfate dosing	2.4	0.9	2.1

Table S4. Comparison of pharmacokinetic parameters for resveratrol and its metabolites. Mice were administered intragastrically either resveratrol or the monosulfates (3:2 mixture of resveratrol-3-*O*- and -4'-*O*-sulfate) at a dose of 120 mg/kg. AUC_{all} values calculated for resveratrol and all the metabolites detected (**A**). Plasma half-life for resveratrol and the sulfate metabolites (**B**). Free resveratrol accounts for 1.9 and 4.4% of the absorbed dose following administration of the sulfates and parent resveratrol, respectively.

	Intracellular concentration of resveratrol species in each incubation (ng/mg cells)	
	Resveratrol sulfates (75 µM)	**Resveratrol (10 µM)**
Resveratrol-3-*O*-sulfate	14.64 ± 3.55	0.30 ± 0.23
Resveratrol-4'-*O*-sulfate	1.84 ± 1.45	<LOD
Resveratrol	0.16 ± 0.05	BLQ
Resveratrol-3-O-glucuronide*	<LOD	<LOD
Resveratrol-4'-O-glucuronide*	0.52 ± 0.16	<LOD
Resveratrol sulfate-glucuronide*	0.29 ± 0.09	<LOD
Resveratrol disulfate*	<LOD	<LOD

**Estimated values, calculated as resveratrol equivalents using a resveratrol standard curve.*

Table S5: Intracellular concentrations in HT-29 cells. Concentration of resveratrol and its metabolites in HT-29 cells measured 24 h after incubation with either a mixture of resveratrol-3-*O*- and -4'-*O*-sulfates (75 µM) or resveratrol (10 µM). Values are the mean ± SD of three independent experiments. Accurate concentrations were determined for resveratrol and each mono-sulfate, but estimates are given for the other metabolites as these were calculated using a resveratrol standard curve. LOD indicates that levels are below the limit of detection (0.0003 ng/mg). BLQ indicates concentrations are below the limit of quantitation, but are detectable and fall within the range of 0.001-0.005 ng/mg cells.